

Deterministic Online Classification: Non-iteratively Reweighted Recursive Least-Squares for Binary Class Rebalancing

Se-In Jang¹

Abstract

Deterministic solutions are becoming more critical for interpretability. Weighted Least-Squares (WLS) has been widely used as a deterministic batch solution with a specific weight design. In the online settings of WLS, exact reweighting is necessary to converge to its batch settings. In order to comply with its necessity, the iteratively reweighted least-squares algorithm is mainly utilized with a linearly growing time complexity which is not attractive for online learning. Due to the high and growing computational costs, an efficient online formulation of reweighted least-squares is desired. We introduce a new deterministic online classification algorithm of WLS with a constant time complexity for binary class rebalancing. We demonstrate that our proposed online formulation exactly converges to its batch formulation and outperforms existing state-of-the-art stochastic online binary classification algorithms in real-world data sets empirically.

1. Introduction

Online learning is an essential step to address large-scale learning (e.g., big data) efficiently and real-time training (e.g., data streaming) in limited computing resources (Bottou & Cun, 2004; Bottou et al., 2018; Cesa-Bianchi & Lugosi, 2006; Hoi et al., 2018; Shalev-Shwartz & Singer, 2007). In designing online learning for classification, a stochastic based approach is mainly explored with several nonlinear loss functions (e.g., step and hinge loss functions). In the stochastic-based online classification, the simplest and most popular architecture is the Perceptron (PE) algorithm (Rosenblatt, 1958) which uses the first-order information obtained from the first-order derivative with a step loss function. The Passive-Aggressive (PA) algorithm (Crammer et al., 2006) is also a successful stochastic-based algorithm that aggressively updates when its hinge loss is non-zero.

¹Gordon Center for Medical Imaging and Center for Advanced Medical Computing and Analysis, Massachusetts General Hospital and Harvard Medical School, Boston, MA, USA. Correspondence to: Se-In Jang <sjang7@mgh.harvard.edu>.

Table 1. An overview of online classification methods.

Algorithms	Learning Type	Reweighting	Imbalance
PE	Stochastic	-	×
PA	Stochastic	-	×
CW	Stochastic	-	×
AROW	Stochastic	-	×
ACOG	Stochastic	-	✓
AR-RLS	Deterministic	Approx.	✓
IR-RLS	Deterministic	Exact	✓
NR-RLS	Deterministic	Exact	✓

The first-order algorithms have paid attention due to their simplicity. However, due to the limited information from the first-order derivative in optimization, the use of the first and second-order information becomes more attractive although it needs more computation than the first-order algorithms (Bottou et al., 2018). One of the most successful second-order algorithms for online classification is the Confidence-Weighted (CW) learning (Dredze et al., 2008), which follows a Gaussian distribution and uses the Kullback–Leibler divergence to stay close to the previous Gaussian distribution. As an improved version of CW, Adaptive Regularization Of Weighted vectors (AROW) learning (Crammer et al., 2009) is developed based on a squared hinge loss function with confidence regularization for handling non-separable data. In (Zhao et al., 2018), an adaptive regularized cost-sensitive online gradient descent algorithm (ACOG) with a weighted sum matrix and a weighted cost metric is presented based on AROW. They assume to give weight to a specific class frequently and aggressively. However, due to this assumption, ACOG cannot be appropriately performed when there are minimal samples for the specific class. The above online learning algorithms well established the classification goals by nonlinear loss functions, which seek to find local minima under the stochastic nature.

Although such stochastic settings have been routinely and successfully applied to online classification problems, logical interpretation of such algorithms was not often convincing due to the inability to settle at the global minimum (Molnar, 2020). The Least-Squares (LS) (Legendre, 1805; Stigler, 1981) is the simplest and most well-known algorithm to obtain a global solution using the squared loss function under the deterministic nature (Willems, 2004). For an online setting of LS, the Recursive Least-Squares (RLS) algorithm was developed for regression analysis (Plackett, 1950; Woodbury, 1950). The RLS algorithm is

not only applied to regression problems but also to the classification problems. However, the objective of RLS could not be accounted as the true objective of classification. In order to achieve the classification objective under the deterministic nature, a quadratic approximation to the step loss function was designed to solve a Total Error Rate minimization problem (TER) (Toh, 2008). The TER's classification objective was achieved by simple class-weight changes based on Weighted Least-Squares (WLS) like cost-sensitive learning (Elkan, 2001; He & Garcia, 2009), where class-weighting plays an essential role in class imbalance problems. Class-weighting has been observed as a valuable way to adjust decision boundaries (Wang et al., 2008; Wu et al., 2010; Scott et al., 2012; Camoriano et al., 2017; Xu et al., 2020).

When making such online settings of WLS, the exact reweighting is necessary to converge to its batch settings. As an exact reweighting formulation, an iteratively reweighted least-squares algorithm was designed without recursive computation (Chartrand & Yin, 2008). In (Camoriano et al., 2017), a recursive reweighting form of the first moment vector was proposed without the inverse of the second moment matrix, which is very significant for the exact convergence to its batch setting. Due to the lack of efficient recursive reweighting formulations of WLS for both the first and second moment matrices, an Approximately Reweighted RLS (AR-RLS) algorithm (Kim et al., 2013) was developed. However, the approximately estimated recursive formulation can cause cumulative approximation errors in optimization. In order to overcome the approximate reweighting, an Iteratively Reweighted RLS (IR-RLS) algorithm (Jang et al., 2017) was then demonstrated for an exact reweighting in a recursive form. However, the iterative inversion of IR-RLS still requires a considerable computational effort with an exponentially growing time complexity. Moreover, due to the limitation of the iterative nature, all the previous samples are also inefficiently stored in memory.

As summarized in Table 1, the main contributions of our work thus include: (i) A new class of an online classification formulation, namely Non-iteratively Reweighted RLS (NR-RLS), which exactly converges to the batch setting of the TER method for deterministic class imbalance classification and achieves a constant time complexity that is preferred for online settings. To the best of our knowledge, this is the first approach that can *non-iteratively, recursively, and exactly* achieve reweighted least-squares in an online setting. Due to this property, this work can be extended to various recursive forms which need a reweighting strategy. (ii) NR-RLS adopts a total-error-rate metric that simultaneously uses two different weights for both positive and negative classes. This helps to address unbalanced data distributions for both classes together. (iii) Accumulation of

the arriving samples efficiently. (iv) Extensive evaluation of the formulation using 31 real-world data sets.

2. Preliminaries

2.1. Least-Squares (LS) Minimization

The Least-Squares (LS) minimization is the most common method for regression and classification problems. The objective function of the LS minimization is based on the sum of squared errors distance function that is more relevant to the regression problems as follows:

$$\text{LS: } J(\mathbf{w}) = \frac{1}{2} \sum_{i=1}^n (y_i - \mathbf{w}^T \mathbf{x}_i)^2 + \frac{b}{2} \|\mathbf{w}\|_2^2, \quad (1)$$

which provides a deterministic closed-form solution as:

$$\mathbf{w} = (\mathbf{X}^T \mathbf{X} + b\mathbf{I})^{-1} \mathbf{X}^T \mathbf{y}, \quad (2)$$

where $\mathbf{X} \in \mathbb{R}^{n \times d}$ is the data matrix, $\mathbf{y} \in \{-1, 1\}$ is the target label vector, n indicates the number of data samples, and d indicates a sample feature dimension. b is a regularization factor and \mathbf{I} is an identity matrix with a similar dimension as $\mathbf{X}^T \mathbf{X}$.

2.2. Minimization for Binary Class Imbalance Learning

Different from the regression objective of LS, in (Toh & Eng, 2008), a classification objective is presented based on a quadratic approximation to the step function for a Total Error Rate (TER) minimization, which can maximize the classification accuracy like cost-sensitive learning and also can handle binary class imbalance classification as follows:

$$\begin{aligned} \text{TER: } J(\mathbf{w}) = & \frac{1}{2n^-} \sum_{i=1}^{n^-} (y_i^- - \mathbf{w}^T \mathbf{x}_i^-)^2 \\ & + \frac{1}{2n^+} \sum_{j=1}^{n^+} (y_j^+ - \mathbf{w}^T \mathbf{x}_j^+)^2 + \frac{b}{2} \|\mathbf{w}\|_2^2, \end{aligned} \quad (3)$$

which also yields a deterministic closed-form solution related to weighted least-squares as:

$$\mathbf{w} = (\mathbf{X}^T \mathbf{W} \mathbf{X} + b\mathbf{I})^{-1} \mathbf{X}^T \mathbf{W} \mathbf{y}, \quad (4)$$

where the superscripts $-$ and $+$ indicate the negative class label and the positive class label respectively. n^- and n^+ respectively indicate the populations of negatively and positively labeled samples. $\mathbf{X} = [\mathbf{X}^-, \mathbf{X}^+]^T$ includes data matrices for negative and positive classes, and $\mathbf{W} = \text{diag} \left(\left[\frac{1}{n^-}, \dots, \frac{1}{n^-}, \frac{1}{n^+}, \dots, \frac{1}{n^+} \right] \right) \in \mathbb{R}^{(n^-+n^+) \times (n^-+n^+)}$ is a class-specific weighting matrix. $\mathbf{y} = [(\tau - \eta), \dots, (\tau - \eta), (\tau + \eta), \dots, (\tau + \eta)] \in \mathbb{R}^{(n^-+n^+)}$ is

the target output, which can be adjusted by changing the decision threshold τ and the offset factor η (see (Toh & Eng, 2008)). Here, $\mathbf{y} = [-1, \dots, -1, 1, \dots, 1]$ is obtained by setting $\tau = 0$ and $\eta = 1$. The prediction outputs for the test set are calculated by $\hat{\mathbf{y}}_{\text{test}} = \mathbf{X}_{\text{test}}\mathbf{w}$. The TER solution is differentiated from the LS solution in the adoption of two different class-specific weights, $\frac{1}{n^-}$ and $\frac{1}{n^+}$, for negative and positive classes. This weight change effectively offers misclassification minimization and class rebalancing together.

2.3. Recursive Least-Squares (RLS)

Recursive least-squares (RLS) learning (Plackett, 1950; Woodbury, 1950; Haykin, 2013) has been frequently utilized as a deterministic closed-form online solution inherited by LS. The RLS coefficient vector \mathbf{w}_t at time t is estimated using

$$\text{RLS: } \mathbf{w}_t = \mathbf{w}_{t-1} + \mathbf{R}_t^{-1} \mathbf{x}_t (y_t - \mathbf{x}_t^T \mathbf{w}_{t-1}), \quad (5)$$

where $\mathbf{x}_t \in \mathbb{R}^d$ and y_t denote respectively the newly arrived sample vector and the output value indexed by time t , and

$$\mathbf{R}_t^{-1} = \mathbf{R}_{t-1}^{-1} - \mathbf{R}_{t-1}^{-1} \mathbf{x}_t (1 + \mathbf{x}_t^T \mathbf{R}_{t-1}^{-1} \mathbf{x}_t)^{-1} \mathbf{x}_t^T \mathbf{R}_{t-1}^{-1} \quad (6)$$

is the recursively accumulated inverse matrix derived from the well-known matrix inversion lemma (Woodbury, 1950; Sherman & Morrison, 1950; Bronštejn & Semendjaev, 2013).

3. Non-iteratively Reweighted Recursive Least-Squares (NR-RLS) for Binary Class Rebalancing

In this section, we will establish a Non-iteratively Reweighted Recursive Least-Squares formulation (NR-RLS), which can precisely calculate a binary class rebalancing loss function in an online setting. The main goal of NR-RLS is to *non-iteratively, recursively and exactly* estimate the coefficient vector \mathbf{w}_t with the two class-specific weights (e.g., $\frac{1}{n^-}$ and $\frac{1}{n^+}$ for the negative and positive classes) which is changed along with the arrival of new samples.

Definition 3.1. The batch solution of (4) can be time-

indexed and rewritten as follows:

$$\begin{aligned} \mathbf{w}_t &= \left(\frac{1}{n_t^-} \mathbf{X}_t^{-T} \mathbf{X}_t^- + \frac{1}{n_t^+} \mathbf{X}_t^{+T} \mathbf{X}_t^+ + b\mathbf{I} \right)^{-1} \\ &\quad \times \left(\frac{1}{n_t^-} \mathbf{X}_t^{-T} \mathbf{y}_t^- + \frac{1}{n_t^+} \mathbf{X}_t^{+T} \mathbf{y}_t^+ \right) \\ &= \left(\frac{1}{n_t^-} \sum_{i=1}^{n_t^-} \mathbf{x}_i^- \mathbf{x}_i^{-T} + \frac{1}{n_t^+} \sum_{j=1}^{n_t^+} \mathbf{x}_j^+ \mathbf{x}_j^{+T} + b\mathbf{I} \right)^{-1} \\ &\quad \times \left(\frac{1}{n_t^-} \sum_{i=1}^{n_t^-} \mathbf{x}_i^- y_i^- + \frac{1}{n_t^+} \sum_{j=1}^{n_t^+} \mathbf{x}_j^+ y_j^+ \right), \end{aligned} \quad (7)$$

where \mathbf{x}_i^- and \mathbf{x}_j^+ respectively indicate the negative and positive labeled data. Next, the two covariance terms within the inverse operation in equation (7) are written as $\mathbf{S}_t^- = \frac{1}{n_t^-} \sum_{i=1}^{n_t^-} \mathbf{x}_i^- \mathbf{x}_i^{-T}$ and $\mathbf{S}_t^+ = \frac{1}{n_t^+} \sum_{j=1}^{n_t^+} \mathbf{x}_j^+ \mathbf{x}_j^{+T}$. (7) can be simplified as

$$\begin{aligned} \mathbf{w}_t &= (\mathbf{S}_t^- + \mathbf{S}_t^+ + b\mathbf{I})^{-1} (\mathbf{z}_t^- + \mathbf{z}_t^+) \\ &= \mathbf{R}_t^{-1} \mathbf{z}_t, \end{aligned} \quad (8)$$

where there is a simple multiplication between the recursive inversion of the weighted second-moment matrix \mathbf{R}_t^{-1} and the recursion of the weighted first-moment vector \mathbf{z}_t .

Theorem 3.2. *The recursive form (8) is identical to the batch form (4) and minimizes the binary class imbalance objective function (3).*

Proof. The proof is in the following subsections. \square

3.1. Derivation of NR-RLS

3.1.1. RECURSIVE INVERSION OF THE SECOND-MOMENT MATRIX \mathbf{R}_t^{-1}

Theorem 3.3. *Suppose \mathbf{R}_t^{-1} consisting of two recursive terms and a constant term. The two recursive matrices, \mathbf{S}_t^- and \mathbf{S}_t^+ , are for accumulation of negative and positive class samples. Since the regularization term $b\mathbf{I}$ is not time-dependent, only the two moment matrices need to be considered in the recursive formulation. Then, $\mathbf{R}_t^{-1} = (\mathbf{S}_t^- + \mathbf{S}_t^+ + b\mathbf{I})^{-1}$ is identical to $\mathbf{R}_t^{-1} = \left(\frac{1}{n_t^-} \mathbf{X}_t^{-T} \mathbf{X}_t^- + \frac{1}{n_t^+} \mathbf{X}_t^{+T} \mathbf{X}_t^+ + b\mathbf{I} \right)^{-1}$.*

Proof. Suppose the newly arriving sample \mathbf{x}_t^- comes from the negative category, then

$$\begin{aligned} \mathbf{S}_t^- &= \frac{n_{t-1}^-}{n_t^-} \underbrace{\sum_{i=1}^{n_{t-1}^-} \frac{1}{n_{t-1}^-} \mathbf{x}_i^- \mathbf{x}_i^{-T}}_{\text{accumulated part, } \mathbf{S}_{t-1}^-} + \frac{1}{n_t^-} \underbrace{\mathbf{x}_t^- \mathbf{x}_t^{-T}}_{\text{new sample}} \\ &= \frac{n_{t-1}^-}{n_t^-} \mathbf{S}_{t-1}^- + \frac{1}{n_t^-} \mathbf{x}_t^- \mathbf{x}_t^{-T}. \end{aligned} \quad (9)$$

Since $\frac{n_{t-1}^-}{n_t^-} = \frac{n_{t-1}^-}{n_{t-1}^-+1} = \left(1 - \frac{1}{n_t^-}\right)$, we have

$$\begin{aligned} \mathbf{S}_t^- &= \left(1 - \frac{1}{n_t^-}\right) \mathbf{S}_{t-1}^- + \frac{1}{n_t^-} \mathbf{x}_t^- \mathbf{x}_t^{-T} \\ &= \mathbf{S}_{t-1}^- - \frac{1}{n_t^-} \mathbf{S}_{t-1}^- + \frac{1}{n_t^-} \mathbf{x}_t^- \mathbf{x}_t^{-T} \\ &= \mathbf{S}_{t-1}^- + \frac{1}{n_t^-} (\mathbf{x}_t^- \mathbf{x}_t^{-T} - \mathbf{S}_{t-1}^-). \end{aligned} \quad (10)$$

On the other hand, if the newly arriving sample \mathbf{x}_t^+ comes from the positive category, then

$$\begin{aligned} \mathbf{S}_t^+ &= \frac{n_{t-1}^+}{n_t^+} \underbrace{\sum_{i=1}^{n_{t-1}^+} \frac{1}{n_{t-1}^+} \mathbf{x}_i^+ \mathbf{x}_i^{+T}}_{\text{accumulated part, } \mathbf{S}_{t-1}^+} + \frac{1}{n_t^+} \underbrace{\mathbf{x}_t^+ \mathbf{x}_t^{+T}}_{\text{new sample}} \\ &= \mathbf{S}_{t-1}^+ - \frac{1}{n_t^+} \mathbf{S}_{t-1}^+ + \frac{1}{n_t^+} \mathbf{x}_t^+ \mathbf{x}_t^{+T} \\ &= \mathbf{S}_{t-1}^+ + \frac{1}{n_t^+} (\mathbf{x}_t^+ \mathbf{x}_t^{+T} - \mathbf{S}_{t-1}^+). \end{aligned} \quad (11)$$

By knowing that the newly arriving sample can only belong to one of the two categories, (10) and (11) are re-written as

$$\begin{aligned} \mathbf{S}_t^- &= \mathbf{S}_{t-1}^- + \beta_t^- (\mathbf{x}_t \mathbf{x}_t^T - \mathbf{S}_{t-1}^-), \\ \mathbf{S}_t^+ &= \mathbf{S}_{t-1}^+ + \beta_t^+ (\mathbf{x}_t \mathbf{x}_t^T - \mathbf{S}_{t-1}^+), \end{aligned} \quad (12)$$

where $\beta_t^- = \frac{(1-y_t)}{2n_t^-}$ and $\beta_t^+ = \frac{(1+y_t)}{2n_t^+}$ are indicators to help a selection of either the negative class or the positive class. Therefore, *the new sample is accumulated* in either \mathbf{S}_t^- or \mathbf{S}_t^+ .

By combining \mathbf{S}_t^- and \mathbf{S}_t^+ in (12), we have

$$\begin{aligned} \mathbf{R}_t &= \mathbf{S}_t^- + \mathbf{S}_t^+ + b\mathbf{I} \\ &= \underbrace{\mathbf{S}_{t-1}^- + \mathbf{S}_{t-1}^+}_{\mathbf{R}_{t-1}} + b\mathbf{I} \\ &\quad - \underbrace{\beta_t^- \mathbf{S}_{t-1}^-}_{\beta_t \mathbf{S}_{t-1}^-} - \underbrace{\beta_t^+ \mathbf{S}_{t-1}^+}_{\beta_t \mathbf{S}_{t-1}^+} + \underbrace{\beta_t^- \mathbf{x}_t \mathbf{x}_t^T + \beta_t^+ \mathbf{x}_t \mathbf{x}_t^T}_{\beta_t \mathbf{x}_t \mathbf{x}_t^T} \\ &= \underbrace{\mathbf{R}_{t-1} - \beta_t \mathbf{S}_{t-1}}_{\mathbf{G}_t} + \beta_t \mathbf{x}_t \mathbf{x}_t^T, \end{aligned} \quad (13)$$

where $\mathbf{S}_{t-1} = \frac{(1-y_t)}{2} \mathbf{S}_{t-1}^- + \frac{(1+y_t)}{2} \mathbf{S}_{t-1}^+$, $\mathbf{x}_t = \frac{(1-y_t)}{2} \mathbf{x}_t^- + \frac{(1+y_t)}{2} \mathbf{x}_t^+$, $\beta_t = \beta_t^- + \beta_t^+$, and $y_t \in \{-1, +1\}$. In order to facilitate the utilization of the existing matrix inversion lemma, (13) is written as two summation terms as follows:

$$\begin{aligned} \mathbf{G}_t &= \mathbf{R}_{t-1} - \beta_t \mathbf{S}_{t-1} \\ \mathbf{R}_t &= \mathbf{G}_t + \beta_t \mathbf{x}_t \mathbf{x}_t^T. \end{aligned} \quad (14)$$

Based on the well-known Sherman-Morrison-Woodbury formulation (Henderson & Searle, 1981):

$$(\mathbf{A} + \mathbf{BCD})^{-1} = \mathbf{A}^{-1} - \mathbf{A}^{-1}(\mathbf{I} + \mathbf{BCDA}^{-1})^{-1}\mathbf{BCDA}^{-1}, \quad (15)$$

the inverses of \mathbf{G}_t and \mathbf{R}_t are given by:

$$\begin{aligned} \mathbf{G}_t^{-1} &= \mathbf{R}_{t-1}^{-1} + \mathbf{R}_{t-1}^{-1}(\mathbf{I} - \beta_t \mathbf{S}_{t-1} \mathbf{R}_{t-1}^{-1})^{-1} \beta_t \mathbf{S}_{t-1} \mathbf{R}_{t-1}^{-1}, \\ \mathbf{R}_t^{-1} &= \mathbf{G}_t^{-1} - \mathbf{G}_t^{-1}(\mathbf{I} + \beta_t \mathbf{x}_t \mathbf{x}_t^T \mathbf{G}_t^{-1})^{-1} \beta_t \mathbf{x}_t \mathbf{x}_t^T \mathbf{G}_t^{-1}, \end{aligned} \quad (16)$$

where \mathbf{G}_t^{-1} is derived based on $(\mathbf{R}_{t-1} - \beta_t \mathbf{S}_{t-1})$ of (14) by putting $\mathbf{A} = \mathbf{R}_{t-1}$, $\mathbf{B} = \mathbf{I}$, $\mathbf{C} = -\beta_t \mathbf{S}_{t-1}$ and $\mathbf{D} = \mathbf{I}$. \mathbf{R}_t^{-1} is derived based on $(\mathbf{G}_t + \beta_t \mathbf{x}_t \mathbf{x}_t^T)$ of (14) by putting $\mathbf{A} = \mathbf{G}_t$, $\mathbf{B} = \beta_t \mathbf{x}_t$, $\mathbf{C} = \mathbf{I}$ and $\mathbf{D} = \mathbf{x}_t^T$. (16) achieves a *non-iteratively and exactly reweighting process* by replacing the old weight, $\frac{1}{n_{t-1}}$ by the new weight, $\frac{1}{n_t}$ for the previously estimated \mathbf{R}_{t-1}^{-1} . \square

3.1.2. RECURSION OF THE FIRST MOMENT VECTOR \mathbf{z}_t

Theorem 3.4. *Suppose \mathbf{z}_t consisting of two recursive terms. The two recursive vectors, \mathbf{z}_t^- and \mathbf{z}_t^+ , are for accumulation of negative and positive class samples. Then, $\mathbf{z}_t = \mathbf{z}_t^- + \mathbf{z}_t^+$ is identical to $\mathbf{z}_t = \frac{1}{n_t} \mathbf{X}_t^{-T} \mathbf{y}_t^- + \frac{1}{n_t} \mathbf{X}_t^{+T} \mathbf{y}_t^+$.*

Proof. Similar to (12), these moment vectors can be easily expressed in terms of their previous estimations as

$$\begin{aligned} \mathbf{z}_t^- &= \mathbf{z}_{t-1}^- + \beta_t^- (\mathbf{x}_t y_t - \mathbf{z}_{t-1}^-), \\ \mathbf{z}_t^+ &= \mathbf{z}_{t-1}^+ + \beta_t^+ (\mathbf{x}_t y_t - \mathbf{z}_{t-1}^+). \end{aligned} \quad (17)$$

\square

3.2. Summary of the proposed NR-RLS algorithm

The proposed NR-RLS algorithm is summarized in the pseudo-code form (see Algorithm 1). The main contribution of the proposed NR-RLS over the existing IR-RLS (Jang et al., 2017) lies on the utilization of a vectorized weight matrix update to replace the iterative nature of the sample-wise weight update. Therefore, the proposed NR-RLS achieves a constant time complexity $\mathcal{O}(2d^2)$ similar to the complexity $\mathcal{O}(d^2)$ of RLS. This solves the linearly growing computational problem of IR-RLS, which has a growing time complexity of $\mathcal{O}(n_t d^2)$ caused by the iterative inversion.

Lemma 3.5. *The proposed NR-RLS classifier asymptotically recover the optimal Bayes classifier and can easily be extended to the multiclass classification.*

Proof. The proof is in the Appendix A and B. \square

4. Experiments

In this section, we perform an empirical evaluation of the proposed Non-iteratively Reweighted Recursive Least-Squares (NR-RLS) based on real-world data sets obtained

Table 2. Summary of the 31 real-world data sets for binary class imbalance classification.

No.	DATA SETS	SIZE	DIMENSION	RATIO	No.	DATA SETS	SIZE	DIMENSION	RATIO
1	MONKS-3	122	6	0.98	17	BLOOD-TRANSFUSION	748	4	0.31
2	MONKS-1	124	6	1.01	18	PIMA-DIABETES	768	8	0.54
3	MONKS-2	169	6	0.62	19	MAMMOGRAPHIC	830	5	0.95
4	WPBC	194	33	0.31	20	TIC-TAC-TOE	958	9	0.53
5	PARKINSONS	195	22	3.15	21	STATLOG-GERMAN	1,000	24	2.34
6	SONAR	208	60	1.16	22	OZONE-EIGHT	1,847	72	0.07
7	SPECTF-HEART	267	44	3.89	23	OZONE-ONE	1,848	72	0.03
8	STATLOG-HEART	270	13	0.80	24	20NEWS-TALK	1,848	3	1.04
9	BUFA-LIVER	345	6	1.39	25	20NEWS-COMP	1,937	3	0.98
10	IONOSPHERE	351	34	0.56	26	20NEWS-SCI	1,971	3	1.01
11	VOTES	435	16	1.60	27	SPAMBASE	4,601	57	0.65
12	MUSK-CLEAN-1	476	166	0.77	28	MUSHROOM	5,644	22	1.62
13	WDBC	569	30	1.69	29	COD-RNA	59,535	8	0.50
14	CREDIT-APP	653	15	1.21	30	IJCNN1	141,691	22	0.11
15	BREAST-CANCER-W	683	9	0.54	31	SKIN-NONSKIN	245,057	3	0.26
16	STATLOG-AUSTRALIAN	690	14	0.81					

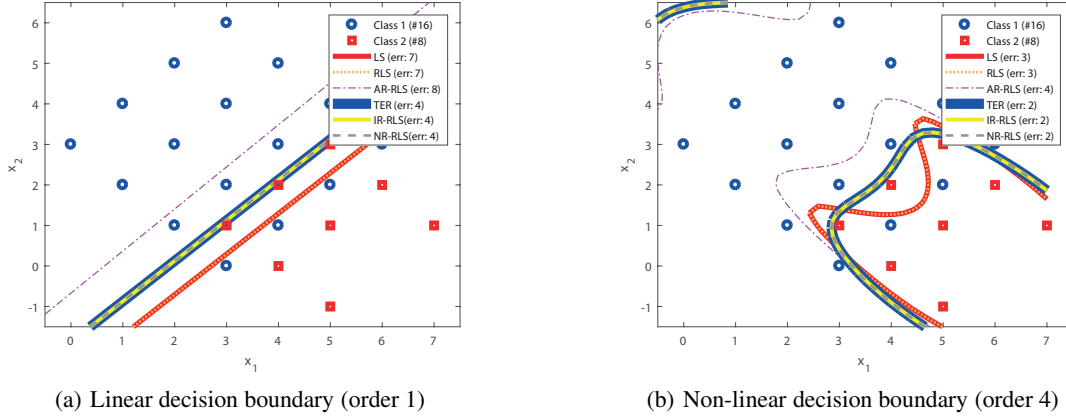


Figure 1. Decision boundaries of the no weighting based solutions (e.g., LS and RLS) and the class-specific weighting based solutions (e.g., TER, AR-RLS, IR-RLS and NR-RLS) at different polynomial orders: (a) at order 1 and (b) at order 4.

Algorithm 1 Non-iteratively Reweighted Recursive Least-Squares

Input: $\mathbf{x}_t \in \mathbb{R}^d$, $y_t \in \{-1, +1\}$
Initialize: $n_0^- = n_0^+ = 0$, $\mathbf{S}_0^- = \mathbf{S}_0^+ = \mathbf{0}$, $\mathbf{z}_0^- = \mathbf{z}_0^+ = \mathbf{0}$,
 $\mathbf{R}_0^{-1} = \frac{1}{b} \mathbf{I}$
for $t = 1, \dots$ **do**
 Update $n_t^- = n_{t-1}^- + \frac{(1-y_t)}{2}$, $n_t^+ = n_{t-1}^+ + \frac{(1+y_t)}{2}$
 Set the following:
 $\beta_t = \beta_t^- + \beta_t^+$, $\beta_t^- = \frac{(1-y_t)}{2n_t^-}$, $\beta_t^+ = \frac{(1+y_t)}{2n_t^+}$
 $\mathbf{S}_{t-1} = \frac{(1-y_t)}{2} \mathbf{S}_{t-1}^- + \frac{(1+y_t)}{2} \mathbf{S}_{t-1}^+$
 Update the following:
 $\mathbf{G}_t^{-1} = \mathbf{R}_{t-1}^{-1} + \mathbf{R}_{t-1}^{-1} (\mathbf{I} - \beta_t \mathbf{S}_{t-1} \mathbf{R}_{t-1}^{-1})^{-1} \beta_t \mathbf{S}_{t-1} \mathbf{R}_{t-1}^{-1}$
 $\mathbf{R}_t^{-1} = \mathbf{G}_t^{-1} - \mathbf{G}_t^{-1} (\mathbf{I} + \beta_t \mathbf{x}_t \mathbf{x}_t^T \mathbf{G}_t^{-1})^{-1} \beta_t \mathbf{x}_t \mathbf{x}_t^T \mathbf{G}_t^{-1}$
 $\mathbf{S}_t^- = \mathbf{S}_{t-1}^- + \beta_t^- (\mathbf{x}_t \mathbf{x}_t^T - \mathbf{S}_{t-1}^-)$,
 $\mathbf{S}_t^+ = \mathbf{S}_{t-1}^+ + \beta_t^+ (\mathbf{x}_t \mathbf{x}_t^T - \mathbf{S}_{t-1}^+)$
 $\mathbf{z}_t^- = \mathbf{z}_{t-1}^- + \beta_t^- (\mathbf{x}_t y_t - \mathbf{z}_{t-1}^-)$,
 $\mathbf{z}_t^+ = \mathbf{z}_{t-1}^+ + \beta_t^+ (\mathbf{x}_t y_t - \mathbf{z}_{t-1}^+)$
 $\mathbf{w}_t = \mathbf{R}_t^{-1} \mathbf{z}_t$, $\mathbf{z}_t = \mathbf{z}_t^- + \mathbf{z}_t^+$
end for

from the public domain (UCI machine learning repository (Lichman, 2013) and LIBSVM website (Chang & Lin, 2011)). The data sets are divided into small, medium and

large scale data groups to observe the impact of data sizes upon online learning. The goals of our experiments are (i) to show the impact of the class-specific weights in a synthetic class imbalance data set; (ii) to observe the convergence between NR-RLS and TER; (iii) to compare the training CPU processing time of NR-RLS with competing algorithms such as RLS, Approximately Reweighted RLS (AR-RLS) and Iteratively Reweighted RLS (IR-RLS); (iv) to compare the accuracy performance of NR-RLS with competing state-of-the-arts such as PErceptron (PE) (Rosenblatt, 1958), online Passive-Aggressive learning (PA) (Crammer et al., 2006), online Confident Weighted learning (CW) (Dredze et al., 2008), Adaptive Regularization Of Weights (AROW) (Crammer et al., 2009) and Adaptive regularized Cost-sensitive Online Gradient descent (ACOG) (Zhao et al., 2018).

4.1. Data sets and experimental setup

In our experiments, twenty small scale data sets ($< 1,000$ samples) are taken from the UCI machine learning repository (Lichman, 2013). Additionally, eight medium scale data sets ($< 10,000$ samples) consist of five data sets from the UCI machine learning repository and three data sets from the 20 Newsgroups which are popular in the NLP community. The sample size of these data set ranges

Table 3. Comparison of average G-means and (ranks).

No.	G-MEAN \pm STD (RANK)							
	THE FIRST-ORDER			THE SECOND-ORDER				
	PE	PA	CW	AROW	ACOG	RLS	AR-RLS	NR-RLS AND IR-RLS
1	0.584 \pm 0.063 (7)	0.593 \pm 0.056 (6)	0.658 \pm 0.073 (5)	0.713 \pm 0.058 (4)	0.533 \pm 0.172 (8)	0.771 \pm 0.036 (1.5)	0.768 \pm 0.048 (3)	0.771 \pm 0.036 (1.5)
2	0.533 \pm 0.069 (7)	0.550 \pm 0.063 (6)	0.571 \pm 0.079 (5)	0.599 \pm 0.040 (4)	0.509 \pm 0.121 (8)	0.659 \pm 0.065 (2)	0.657 \pm 0.058 (3)	0.662 \pm 0.061 (1)
3	0.472 \pm 0.046 (5)	0.475 \pm 0.046 (4)	0.514 \pm 0.061 (1)	0.246 \pm 0.192 (7)	0.218 \pm 0.191 (8)	0.330 \pm 0.108 (6)	0.492 \pm 0.088 (3)	0.511 \pm 0.056 (2)
4	0.440 \pm 0.093 (5)	0.440 \pm 0.075 (6)	0.522 \pm 0.087 (4)	0.285 \pm 0.230 (7)	0.114 \pm 0.176 (8)	0.639 \pm 0.081 (3)	0.687 \pm 0.058 (2)	0.688 \pm 0.047 (1)
5	0.508 \pm 0.058 (6)	0.470 \pm 0.045 (7)	0.657 \pm 0.044 (4)	0.584 \pm 0.103 (5)	0.234 \pm 0.254 (8)	0.751 \pm 0.067 (3)	0.772 \pm 0.055 (2)	0.775 \pm 0.050 (1)
6	0.548 \pm 0.039 (6)	0.529 \pm 0.051 (8)	0.675 \pm 0.050 (4)	0.674 \pm 0.049 (5)	0.542 \pm 0.122 (7)	0.702 \pm 0.039 (3)	0.710 \pm 0.040 (2)	0.729 \pm 0.038 (1)
7	0.423 \pm 0.070 (5)	0.407 \pm 0.072 (6)	0.540 \pm 0.074 (3)	0.077 \pm 0.112 (7)	0.046 \pm 0.098 (8)	0.450 \pm 0.103 (4)	0.630 \pm 0.073 (2)	0.649 \pm 0.055 (1)
8	0.576 \pm 0.033 (7)	0.540 \pm 0.031 (8)	0.721 \pm 0.039 (5)	0.786 \pm 0.029 (4)	0.644 \pm 0.176 (6)	0.820 \pm 0.028 (3)	0.821 \pm 0.026 (2)	0.823 \pm 0.029 (1)
9	0.500 \pm 0.028 (6)	0.498 \pm 0.028 (7)	0.577 \pm 0.045 (4)	0.543 \pm 0.061 (5)	0.158 \pm 0.192 (8)	0.629 \pm 0.024 (3)	0.632 \pm 0.026 (2)	0.639 \pm 0.031 (1)
10	0.532 \pm 0.033 (6)	0.509 \pm 0.037 (7)	0.762 \pm 0.022 (4)	0.731 \pm 0.039 (5)	0.494 \pm 0.101 (3)	0.786 \pm 0.048 (3)	0.795 \pm 0.041 (2)	0.796 \pm 0.040 (1)
11	0.815 \pm 0.025 (8)	0.837 \pm 0.025 (7)	0.909 \pm 0.023 (5)	0.925 \pm 0.014 (4)	0.863 \pm 0.079 (6)	0.944 \pm 0.011 (3)	0.946 \pm 0.012 (1.5)	0.946 \pm 0.012 (1.5)
12	0.503 \pm 0.036 (6)	0.488 \pm 0.035 (7)	0.735 \pm 0.025 (5)	0.736 \pm 0.026 (4)	0.483 \pm 0.217 (8)	0.750 \pm 0.028 (3)	0.754 \pm 0.025 (2)	0.806 \pm 0.022 (1)
13	0.767 \pm 0.027 (7)	0.718 \pm 0.018 (8)	0.939 \pm 0.011 (3)	0.934 \pm 0.011 (5)	0.768 \pm 0.145 (6)	0.938 \pm 0.014 (4)	0.951 \pm 0.015 (2)	0.956 \pm 0.011 (1)
14	0.645 \pm 0.058 (7)	0.572 \pm 0.028 (8)	0.765 \pm 0.023 (5)	0.845 \pm 0.015 (4)	0.684 \pm 0.168 (6)	0.869 \pm 0.012 (1.5)	0.868 \pm 0.013 (3)	0.869 \pm 0.012 (1.5)
15	0.916 \pm 0.017 (7)	0.921 \pm 0.013 (6)	0.934 \pm 0.019 (5)	0.948 \pm 0.009 (4)	0.834 \pm 0.096 (8)	0.950 \pm 0.009 (3)	0.957 \pm 0.009 (1)	0.956 \pm 0.009 (2)
16	0.619 \pm 0.038 (7)	0.541 \pm 0.030 (8)	0.764 \pm 0.022 (5)	0.850 \pm 0.013 (4)	0.738 \pm 0.115 (6)	0.864 \pm 0.013 (1.5)	0.863 \pm 0.014 (3)	0.864 \pm 0.013 (1.5)
17	0.485 \pm 0.046 (4)	0.456 \pm 0.040 (5)	0.526 \pm 0.057 (3)	0.237 \pm 0.100 (7)	0.103 \pm 0.139 (8)	0.286 \pm 0.043 (6)	0.682 \pm 0.023 (2)	0.685 \pm 0.022 (1)
18	0.555 \pm 0.022 (6)	0.502 \pm 0.021 (7)	0.625 \pm 0.021 (5)	0.667 \pm 0.035 (4)	0.435 \pm 0.224 (8)	0.698 \pm 0.021 (3)	0.739 \pm 0.017 (2)	0.742 \pm 0.014 (1)
19	0.598 \pm 0.019 (7)	0.499 \pm 0.031 (8)	0.722 \pm 0.023 (5)	0.798 \pm 0.010 (4)	0.603 \pm 0.218 (6)	0.813 \pm 0.019 (2.5)	0.814 \pm 0.017 (1)	0.813 \pm 0.019 (2.5)
20	0.505 \pm 0.025 (5)	0.505 \pm 0.017 (4)	0.511 \pm 0.024 (3)	0.334 \pm 0.093 (7)	0.097 \pm 0.137 (8)	0.427 \pm 0.049 (6)	0.576 \pm 0.016 (2)	0.577 \pm 0.021 (1)
21	0.601 \pm 0.027 (6)	0.591 \pm 0.028 (8)	0.594 \pm 0.028 (7)	0.622 \pm 0.036 (4)	0.616 \pm 0.052 (5)	0.638 \pm 0.029 (3)	0.714 \pm 0.021 (2)	0.715 \pm 0.019 (1)
22	0.364 \pm 0.066 (4)	0.296 \pm 0.061 (5)	0.571 \pm 0.045 (3)	0.072 \pm 0.106 (6)	0.000 \pm 0.000 (8)	0.007 \pm 0.029 (7)	0.807 \pm 0.033 (2)	0.820 \pm 0.018 (1)
23	0.240 \pm 0.104 (4)	0.161 \pm 0.101 (5)	0.423 \pm 0.100 (3)	0.009 \pm 0.041 (6.5)	0.009 \pm 0.041 (6.5)	0.000 \pm 0.000 (8)	0.788 \pm 0.036 (2)	0.819 \pm 0.035 (1)
24	0.500 \pm 0.014 (1)	0.498 \pm 0.017 (2)	0.481 \pm 0.070 (4)	0.456 \pm 0.042 (5)	0.326 \pm 0.171 (8)	0.359 \pm 0.194 (7)	0.374 \pm 0.178 (6)	0.483 \pm 0.016 (3)
25	0.574 \pm 0.013 (6)	0.548 \pm 0.013 (7)	0.477 \pm 0.096 (8)	0.679 \pm 0.017 (4)	0.633 \pm 0.074 (5)	0.695 \pm 0.039 (1.5)	0.688 \pm 0.050 (3)	0.695 \pm 0.039 (1.5)
26	0.714 \pm 0.014 (7)	0.689 \pm 0.012 (8)	0.722 \pm 0.065 (6)	0.850 \pm 0.015 (4)	0.745 \pm 0.055 (5)	0.892 \pm 0.017 (1.5)	0.877 \pm 0.032 (3)	0.892 \pm 0.017 (1.5)
27	0.610 \pm 0.036 (8)	0.630 \pm 0.008 (7)	0.865 \pm 0.007 (4)	0.869 \pm 0.006 (3)	0.671 \pm 0.119 (6)	0.864 \pm 0.010 (5)	0.899 \pm 0.007 (2)	0.900 \pm 0.006 (1)
28	0.679 \pm 0.022 (7)	0.510 \pm 0.010 (8)	0.984 \pm 0.001 (1)	0.916 \pm 0.009 (5)	0.800 \pm 0.081 (6)	0.932 \pm 0.009 (4)	0.949 \pm 0.004 (3)	0.950 \pm 0.003 (2)
29	0.763 \pm 0.002 (6)	0.718 \pm 0.005 (7)	0.863 \pm 0.002 (5)	0.930 \pm 0.001 (3)	0.714 \pm 0.304 (8)	0.928 \pm 0.001 (4)	0.939 \pm 0.001 (2)	0.940 \pm 0.001 (1)
30	0.631 \pm 0.004 (4)	0.627 \pm 0.005 (5)	0.692 \pm 0.004 (3)	0.508 \pm 0.009 (6)	0.173 \pm 0.085 (8)	0.301 \pm 0.007 (7)	0.858 \pm 0.004 (2)	0.859 \pm 0.004 (1)
31	0.768 \pm 0.002 (7)	0.783 \pm 0.002 (6)	0.454 \pm 0.015 (8)	0.899 \pm 0.001 (4)	0.784 \pm 0.342 (5)	0.904 \pm 0.001 (3)	0.957 \pm 0.000 (2)	0.958 \pm 0.000 (1)
AVG.	0.580 \pm 0.037 (5.94)	0.552 \pm 0.033 (6.48)	0.670 \pm 0.040 (4.35)	0.673 \pm 0.050 (4.85)	0.470 \pm 0.147 (7.07)	0.664 \pm 0.037 (3.74)	0.773 \pm 0.034 (2.29)	0.783 \pm 0.024 (1.32)

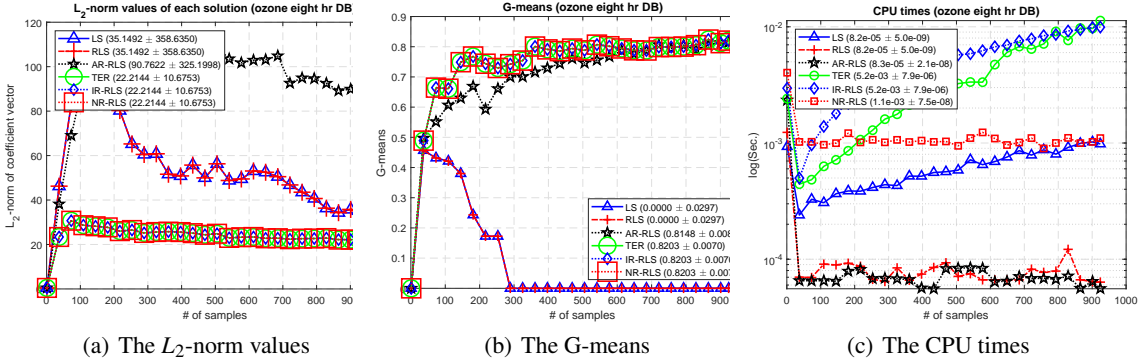


Figure 2. Comparisons of (a) the L_2 -norm values, (b) the G-means and (c) the CPU times among LS, RLS, TER, AR-RLS, IR-RLS and NR-RLS plotted over different number of training samples for the ‘Ozone-eight’ data set. Each bracket in legends indicates a mean value and its standard deviation over the number of samples.

from 122 to 245,057 samples. The data imbalance ratio is calculated by $\frac{n^+}{n^-}$. In addition to these two groups of data, three large scale data sets from the LIBSVM website (Chang & Lin, 2011) are included in this study. In (Lu et al., 2016; Jian et al., 2017; Hu et al., 2015; Ito et al., 2017), these data sets are considered as the large scale data sets ($> 50,000$ samples). The input data is normalized to the range $[0, 1]$. Table 2 summarizes the attributes of the total 31 data sets used in our study. For performance comparison with representative online algorithms, our proposed NR-RLS is compared with PE (Rosenblatt, 1958), PA (Crammer et al., 2006), CW (Dredze et al., 2008), AROW (Crammer et al., 2009), ACOG (Zhao et al., 2018), RLS (Haykin, 2013), AR-RLS (Kim et al., 2013) and IR-RLS (Jang et al., 2017).

Similar to (Kim et al., 2012), our experiments are recorded using ten runs of 2-fold cross-validations for all compared algorithms. We adopt a G -mean matrix (He & Garcia,

2009) which evaluates the degree of inductive bias in terms of a ratio of the positive and negative accuracies as follows:

$$G\text{-mean} = \sqrt{\frac{TP}{TP+FN} \times \frac{TN}{TN+FP}}$$

The average G -means for the unseen test data are recorded. In the class-specific weighting based classifiers, namely TER, AR-RLS, IR-RLS and NR-RLS, there are two parameters: the class-specific weight and the regularization factor b . The RLS classifier has one parameter b . Here, the regularization setting b is set at a small value of $b = 10^{-4}$ following (Kim et al., 2012; Toh & Tan, 2014) since the main objective of this setting is to stabilize the least-squares solution. The class-specific weight is varied according to (Toh & Eng, 2008). By setting $n_i^- = 1$ and $n_i^+ = 1$ without its update, the proposed NR-RLS can take the balanced weight setting, heading to the LS objective. To address the nonlinear input-output relationship, the multivariate polynomial model is adopted at different polynomial orders $r \in \{1, 2, \dots, 6\}$.

4.2. Comprehensive analysis of the no weighting and the class-specific reweighting based solutions

In order to observe the effectiveness of the class-specific reweighting for binary class rebalancing, the class-specific reweighting based TER, AR-RLS, IR-RLS and NR-RLS are compared with the no weighting based LS and RLS.

4.2.1. THE IMPACT OF CLASS-SPECIFIC WEIGHTS IN CLASS IMBALANCE LEARNING

In order to observe the difference between LS and TER in a class imbalance problem, Fig. 1 illustrates the decision boundaries on a synthetic example consisting of 24 unbalanced discrete data points (i.e., 8 negative samples and 16 positive samples) with 7 overlapping data points. The decision boundaries are drawn in two different order polynomials (e.g., the first and fourth orders). Fig. 1(a) shows 7 error counts for ‘LS and RLS’, 4 error counts for ‘TER, IR-RLS and NR-RLS’ and 8 error counts for ‘AR-RLS’ in the first order polynomial. The exact reweighting based TER, IR-RLS and NR-RLS achieve lower error counts than the no weighting based solutions and the approximate reweighting based AR-RLS. Fig. 1(b) also shows the error counts in the fourth-order polynomial. The error counts for ‘LS and RLS’, ‘TER, IR-RLS and NR-RLS’ and ‘AR-RLS’ are given by 3, 2 and 4. Similarly, the exact reweighting based TER, IR-RLS and NR-RLS are seen to be the best performer compared to all the other solutions. In Fig. 1, the equality between the batch and online settings can be found in (i) LS and RLS, (ii) TER, IR-RLS and NR-RLS, whereas the inequality remains between TER and AR-RLS.

4.2.2. OBSERVING THE CONVERGENCE TRENDS

In order to observe the convergence trends of the batch and recursive formulations using real-world data, the ‘Ozone-eight’ data set from the UCI repository (Lichman, 2013) is adopted for this investigation. Fig. 2(a) shows the L_2 -norm of the coefficient vectors for each algorithm. In this figure, the average L_2 -norm values show that IR-RLS and NR-RLS converge to the batch setting of TER while AR-RLS shows a different convergence. Similarly, RLS shows the same convergence with the batch setting of LS. In the Appendix C, we give a figure which includes each value of the coefficient vectors.

Fig. 2(b) shows the estimation trends of the compared algorithms according to each arrival of training samples. We observe that each group of ‘TER, IR-RLS and NR-RLS’ and ‘LS and RLS’ achieves the same G -mean and the same standard deviation, whereas AR-RLS shows the different G -mean and standard deviation from the exact reweighting group. This also verifies that NR-RLS is converged to TER. Due to the exact convergence of the TER objective, IR-RLS and NR-RLS show a better G -mean perfor-

mance than the approximate reweighting based AR-RLS. Since the ‘Ozone-eight’ data set is highly imbalanced with its ratio, 0.07, shown in Table 2, the no weighting based LS and RLS cannot classify one class completely. In Fig. 2(a) and (b), the exact reweighting based TER, IR-RLS, and NR-RLS show a lower standard deviation than LS, RLS, and AR-RLS.

4.2.3. COMPARING THE CPU PROCESSING TIME

The ‘Ozone-eight’ data set is again used for comparing the training computational time. Fig. 2(c) shows the average CPU times of LS, RLS, TER, AR-RLS, IR-RLS, and NR-RLS over 10 runs along with each arriving training sample. Due to the batch mode and iterative reweighting settings, the computational times of LS, TER and IR-RLS are linearly growing according to the increasing number of samples. Different from LS, TER, and IR-RLS, the non-growing computational times of RLS, AR-RLS, and NR-RLS are observed. Similar to Fig. 2, we provide all the corresponding figures for each data set in the Appendix D.

4.3. Performance evaluation

4.3.1. COMPARING G -MEAN AND CPU TIME PERFORMANCES AMONG THE STATE-OF-THE-ARTS

Table 3 shows the average G -mean results with its standard deviation and ranks of the 31 data sets. In the Appendix E, highly imbalanced data sets (e.g., Ozone and IJCNN) are highlighted. The G -mean and CPU time values are recorded based on 10 runs of 2-fold cross-validation. As competing state-of-the-arts, two first-order algorithms such as PE (Rosenblatt, 1958) and PA (Crammer et al., 2006) are included, and five second-order algorithms, namely CW (Dredze et al., 2008), AROW (Crammer et al., 2009), ACOG (Zhao et al., 2018), RLS (Haykin, 2013), AR-RLS (Kim et al., 2013), and IR-RLS (Jang et al., 2017) are adopted.

Several observations are gathered for this experiment. Firstly, the second-order solutions show higher average G -means than the first-order solutions. This is due to the use of more information than the first-order information in the update rules. This consistent observation can also be found in (Dredze et al., 2008; Crammer et al., 2009; Hao et al., 2018). Secondly, the exact reweighting based solutions namely, NR-RLS and IR-RLS show the highest average G -mean performance than all the other solutions. The main reason is due to the direct optimization of the classification error goal with the class imbalance classification design. Additionally, NR-RLS and IR-RLS give the lowest standard deviation than all the state-of-the-art methods.

Table 4 shows the average CPU time on the 31 data sets.

Table 4. Comparison of average training CPU times in seconds

No.	TRAINING CPU TIMES IN SECONDS							
	THE FIRST-ORDER				THE SECOND-ORDER			
	PE	PA	CW	AROW	RLS	AR-RLS	IR-RLS	NR-RLS
1	0.0052	0.0026	0.0021	0.0024	0.0053	0.0099	0.0388	0.0254
2	0.0014	0.0013	0.0020	0.0023	0.0007	0.0007	0.0170	0.0068
3	0.0017	0.0019	0.0028	0.0034	0.0009	0.0010	0.0265	0.0036
4	0.0021	0.0021	0.0039	0.0046	0.0016	0.0018	0.0658	0.0123
5	0.0019	0.0021	0.0033	0.0040	0.0014	0.0017	0.0539	0.0087
6	0.0023	0.0022	0.0063	0.0071	0.0035	0.0045	0.2497	0.0382
7	0.0035	0.0034	0.0080	0.0110	0.0036	0.0038	0.2218	0.0307
8	0.0028	0.0030	0.0046	0.0053	0.0014	0.0016	0.0785	0.0096
9	0.0037	0.0038	0.0058	0.0071	0.0018	0.0020	0.1019	0.0081
10	0.0035	0.0041	0.0061	0.0078	0.0031	0.0034	0.2303	0.0347
11	0.0051	0.0050	0.0067	0.0086	0.0027	0.0028	0.1770	0.0126
12	0.0057	0.0084	0.0619	0.0725	0.0433	0.0438	5.5455	0.4465
13	0.0050	0.0058	0.0079	0.0104	0.0046	0.0115	0.4944	0.0305
14	0.0074	0.0079	0.0096	0.0131	0.0034	0.0039	0.3622	0.0160
15	0.0064	0.0064	0.0085	0.0105	0.0037	0.0041	0.3938	0.0139
16	0.0064	0.0074	0.0099	0.0126	0.0038	0.0053	0.4389	0.0190
17	0.0073	0.0074	0.0126	0.0139	0.0035	0.0041	0.4350	0.0142
18	0.0074	0.0088	0.0109	0.0154	0.0050	0.0044	0.5167	0.0152
19	0.0083	0.0083	0.0111	0.0152	0.0040	0.0049	0.5469	0.0145
20	0.0095	0.0096	0.0149	0.0178	0.0052	0.0058	0.7547	0.0215
21	0.0109	0.0111	0.0233	0.0267	0.1160	0.1293	6.1132	1.5705
22	0.0164	0.0173	0.0398	0.0599	0.0503	0.0444	17.9072	0.4350
23	0.0168	0.0163	0.0344	0.0645	0.0437	0.0448	17.5479	0.4225
24	0.0211	0.0212	0.0364	0.0324	0.0095	0.0121	2.1149	0.0672
25	0.0204	0.0218	0.031	0.0336	0.0136	0.0184	1.9262	0.0592
26	0.0216	0.0219	0.0302	0.0339	0.0103	0.0133	1.9603	0.0571
27	0.0417	0.0493	0.0924	0.1331	0.0816	0.0891	94.5412	0.7049
28	0.0572	0.0610	0.0641	0.1220	0.0580	0.0668	37.2190	0.2729
29	0.5827	0.6056	0.7635	1.0081	0.6249	0.6699	2402.4486	1.6872
30	1.3512	1.3686	1.9197	2.4948	2.5199	3.0872	23977.8040	8.3815
31	2.2627	2.4008	2.9559	4.3889	3.1734	3.4330	39724.2624	6.4619
AVG	0.1451	0.1515	0.1997	0.2788	0.2195	0.2493	2138.5353	0.6742



Figure 3. Statistical significance among the averaged (a) G -means and (b) computational times of the online algorithms according to the Nemenyi test. The connected algorithms by the Critical Difference (CD) are those that their differences in performance are of no statistical significance.

The computational time of NR-RLS is much faster than IR-RLS. The main reason is the replacement of the iterative reweighting with the single-step vectorized reweighting. The computational times of the first-order algorithms are seen to be faster than the second-order methods.

Friedman tests (see (Demšar, 2006)) on the G -mean and CPU time comparisons reject the null hypothesis that all eight compared algorithms are statistically equivalent. These are followed by Nemenyi plots as a post-hoc analysis to show the groups of connected algorithms that are not significantly different at $p = 0.05$. In Fig. 3(a), the Nemenyi plot for the G -mean rank shows six groups of algorithm similarity namely, (i) IR-RLS–NR-RLS–AR-RLS, (ii) AR-RLS–RLS, (iii) RLS–CW–AROW, (iv) CW–AROW–PE, (v) AROW–PE–PA, and (vi) PE–PA–ACOG. In the first group, NR-RLS and IR-RLS achieve the highest rank and significantly differ from all the other algorithms in the lowly-ranked groups. NR-RLS and IR-RLS show the higher G -mean performance than all the other algorithms. Since NR-RLS–IR-RLS is not overlapped between the first and second groups, NR-RLS–IR-RLS are

seen to be the best performer. In Fig. 3(b), the Nemenyi plot for the computational rank also shows six groups of algorithm similarity, namely (i) RLS–PE–PA–AR-RLS, (ii) PE–PA–AR-RLS–CW, (iii) CW–AROW, (iv) AROW–ACOG, (v) ACOG–NR-RLS, and (vi) NR-RLS–IR-RLS. The proposed NR-RLS is overlapped between the two lowly-ranked groups.

Here, we summarize our observations: (i) In terms of the G -mean performance, the equivalence between TER and NR-RLS is observed. The exact reweighting based NR-RLS outperformed each of the approximate reweighting based AR-RLS, the no weighting based RLS, and the stochastic based solutions such as PE, PA, CW, AROW, and ACOG with statistical significance. (ii) In terms of the computational time, the non-growing computational trend of NR-RLS is observed whereas IR-RLS showed the growing computational trend. NR-RLS is seen to be slower than the first-order and the second-order solutions but comparable to them.

5. Conclusion

This paper presented a new deterministic online learning formulation of the weighted least-squares for binary class rebalancing. Specifically, we proposed a non-iteratively reweighted recursive least-squares algorithm which is designed to replace the old weights with the new ones. We showed that the proposed online formulation converged to the batch setting for binary class imbalance classification and achieved the constant time complexity. We also showed that the proposed algorithm outperformed the state-of-the-art online binary classification algorithms effectively and efficiently. In the future, we will extend this formulation to nonlinear classifiers in a reproducing kernel Hilbert space.

References

- Bottou, L. and Cun, Y. L. Large scale online learning. In *Advances in neural information processing systems*, pp. 217–224, 2004.
- Bottou, L., Curtis, F. E., and Nocedal, J. Optimization methods for large-scale machine learning. *Siam Review*, 60(2):223–311, 2018.
- Bronštejn, I. N. and Semendjaev, K. A. *Handbook of mathematics*. Springer, 2013.
- Camoriano, R., Pasquale, G., Ciliberto, C., Natale, L., Rosasco, L., and Metta, G. Incremental robot learning of new objects with fixed update time. In *2017 IEEE International Conference on Robotics and Automation (ICRA)*, pp. 3207–3214. IEEE, 2017.
- Cesa-Bianchi, N. and Lugosi, G. *Prediction, learning, and games*. Cambridge university press, 2006.
- Chang, C.-C. and Lin, C.-J. LIBSVM: A library for support vector machines. *ACM Transactions on Intelligent Systems and Technology*, 2:27:1–27:27, 2011. Software available at <http://www.csie.ntu.edu.tw/~cjlin/libsvm>.
- Chartrand, R. and Yin, W. Iteratively reweighted algorithms for compressive sensing. In *IEEE International Conference on Acoustics, Speech and Signal Processing*, pp. 3869–3872. IEEE, 2008.
- Crammer, K., Dekel, O., Keshet, J., Shalev-Shwartz, S., and Singer, Y. Online passive-aggressive algorithms. *Journal of Machine Learning Research*, 7(Mar):551–585, 2006.
- Crammer, K., Kulesza, A., and Dredze, M. Adaptive regularization of weight vectors. In *Advances in neural information processing systems*, pp. 414–422, 2009.
- Demšar, J. Statistical comparisons of classifiers over multiple data sets. *Journal of Machine learning research*, 7 (Jan):1–30, 2006.
- Dredze, M., Crammer, K., and Pereira, F. Confidence-weighted linear classification. In *International Conference on Machine Learning*, pp. 264–271. ACM, 2008.
- Elkan, C. The foundations of cost-sensitive learning. In *International joint conference on artificial intelligence*, volume 17, pp. 973–978. Lawrence Erlbaum Associates Ltd, 2001.
- Hao, S., Lu, J., Zhao, P., Zhang, C., Hoi, S. C., and Miao, C. Second-order online active learning and its applications. *IEEE Transactions on Knowledge and Data Engineering*, 30(7):1338–1351, 2018.
- Haykin, S. O. *Adaptive filter theory*. Prentice-Hall, fifth edition, 2013.
- He, H. and Garcia, E. A. Learning from imbalanced data. *IEEE Transactions on Knowledge and Data Engineering*, 21(9):1263–1284, 2009.
- Henderson, H. V. and Searle, S. R. On deriving the inverse of a sum of matrices. *SIAM Review*, 23(1):53–60, 1981.
- Hoi, S. C. H., Sahoo, D., Lu, J., and Zhao, P. Online learning: A comprehensive survey. *arXiv preprint arXiv:1802.02871*, 2018.
- Hu, Z., Lin, M., and Zhang, C. Dependent online kernel learning with constant number of random fourier features. *IEEE transactions on neural networks and learning systems*, 26(10):2464–2476, 2015.
- Ito, N., Takeda, A., and Toh, K.-C. A unified formulation and fast accelerated proximal gradient method for classification. *Journal of Machine Learning Research*, 18(16):1–49, 2017.
- Jang, S.-I., Tan, G.-C., Toh, K.-A., and Teoh, A. B. J. Online heterogeneous face recognition based on total error rate minimization. *IEEE Transactions on Systems, Man, and Cybernetics: Systems*, 2017.
- Jian, L., Shen, S., Li, J., Liang, X., and Li, L. Budget online learning algorithm for least squares svm. *IEEE transactions on neural networks and learning systems*, 2017.
- Kim, Y., Toh, K.-A., Teoh, A. B. J., Eng, H.-L., and Yau, W.-Y. An online auc formulation for binary classification. *Pattern Recognition*, 45(6):2266–2279, 2012.
- Kim, Y., Toh, K.-A., Teoh, A. B. J., Eng, H.-L., and Yau, W.-Y. An online learning network for biometric scores fusion. *Neurocomputing*, 102:65–77, 2013.

- Legendre, A.-M. *Nouvelles méthodes pour la détermination des orbites des comètes (New methods for determining the orbits of comets)*. Number 1. Firmin Didot, 1805.
- Lichman, M. UCI machine learning repository, 2013. URL <http://archive.ics.uci.edu/ml>.
- Lu, J., Hoi, S. C., Wang, J., Zhao, P., and Liu, Z.-Y. Large scale online kernel learning. *Journal of Machine Learning Research*, 17(47):1, 2016.
- Molnar, C. *Interpretable machine learning*. Lulu. com, 2020.
- Plackett, R. L. Some theorems in least squares. *Biometrika*, 37(1-2):149–157, 1950.
- Rosenblatt, F. The perceptron: A probabilistic model for information storage and organization in the brain. *Psychological review*, 65(6):386, 1958.
- Scott, C. et al. Calibrated asymmetric surrogate losses. *Electronic Journal of Statistics*, 6:958–992, 2012.
- Shalev-Shwartz, S. and Singer, Y. *Online learning: Theory, algorithms, and applications*. 2007.
- Sherman, J. and Morrison, W. J. Adjustment of an inverse matrix corresponding to a change in one element of a given matrix. *The Annals of Mathematical Statistics*, 21(1):124–127, 1950.
- Stigler, S. M. Gauss and the invention of least squares. *The Annals of Statistics*, pp. 465–474, 1981.
- Toh, K.-A. Deterministic neural classification. *Neural computation*, 20(6):1565–1595, 2008.
- Toh, K.-A. and Eng, H.-L. Between classification-error approximation and weighted least-squares learning. *IEEE Transactions on Pattern Analysis and Machine Intelligence*, 30(4):658–669, 2008.
- Toh, K.-A. and Tan, G.-C. Exploiting the relationships among several binary classifiers via data transformation. *Pattern Recognition*, 47(3):1509–1522, 2014.
- Wang, J., Shen, X., and Liu, Y. Probability estimation for large-margin classifiers. *Biometrika*, 95(1):149–167, 2008.
- Willems, J. C. Deterministic least squares filtering. *Journal of econometrics*, 118(1-2):341–373, 2004.
- Woodbury, M. A. Inverting modified matrices. *Memorandum report*, 42:4, 1950.
- Wu, Y., Zhang, H. H., and Liu, Y. Robust model-free multiclass probability estimation. *Journal of the American Statistical Association*, 105(489):424–436, 2010.
- Xu, Z., Dan, C., Khim, J., and Ravikumar, P. Class-weighted classification: Trade-offs and robust approaches. In *International Conference on Machine Learning*, pp. 10544–10554. PMLR, 2020.
- Zhao, P., Zhang, Y., Wu, M., Hoi, S. C., Tan, M., and Huang, J. Adaptive cost-sensitive online classification. *IEEE Transactions on Knowledge and Data Engineering*, 31(2):214–228, 2018.

Appendix

Our appendices contain additional details which are omitted from the main text.

In Appendix A, we introduce the relationship between the optimal Bayes classifier and the Least-Squares (LS) classifier. We also show the weighted version of the optimal Bayes classifier and then build the relationship among the weighted optimal Bayes classifier, the Weighted Least-Squares (WLS) classifier and the Total-Error-Rate (TER) classifier.

In Appendix B, we show that the proposed NR-RLS can easily be extended to the multiclass classification.

In Appendix C, we show the learned coefficient vectors of LS, Recursive LS (RLS), TER, Approximately Reweighted RLS (AR-RLS), Iteratively Reweighted RLS (IR-RLS), Non-iteratively Reweighted RLS (NR-RLS) to experimentally provide the convergence results between the batch and online settings on the Mushroom data set which has enough numbers of feature dimension and data samples to show a good presentation.

In Appendix D, we provide all the figures which show L_2 -norm, G -mean and CPU time values for each data set. In the main text, we only showed the figure for the ozone-eight data set as a representative example.

In Appendix E, we highlight the data sets highly imbalanced.

A. Relationship with the optimal Bayes classifier

Consider a binary classification problem with a finite set of observations $\{\mathbf{x}_i, y_i\}_i^n$, where \mathbf{x} and y are the input and the output that randomly sampled according to a distribution p over $\mathcal{X} \times \{-1, 1\}$. The overall classification error can be minimized by the optimal Bayes classifier as follows:

$$f_{Bayes}^* = \arg \min_{f_{Bayes}: \mathcal{X} \rightarrow \{-1, 1\}} \int_{\mathcal{X} \times \{-1, 1\}} \mathbf{1}(f_{Bayes}(\mathbf{x}) - y) dp(\mathbf{x}, y), \quad (18)$$

where $\mathbf{1}(\cdot) : \mathbb{R} \rightarrow \{0, 1\}$ is the binary function. The optimal Bayes classifier satisfies the following equation:

$$f_{Bayes}^*(\mathbf{x}) = \begin{cases} 1 & \text{if } p(1|\mathbf{x}) > p(-1|\mathbf{x}) \\ -1 & \text{otherwise} \end{cases}. \quad (19)$$

Since large scale data sets are needed for good estimation of $p(y|\mathbf{x})$, a good surrogate method is required for a good feasible solution in practice. The Least-Squares (LS) minimization is a well-known method to asymptotically recover the optimal Bayes classifier as follows:

$$f_{LS}^* = \arg \min_{f_{LS}: \mathcal{X} \rightarrow \mathbb{R}} \int_{\mathcal{X} \times \{-1, 1\}} (y - f_{LS}(\mathbf{x}))^2 dp(\mathbf{x}, y). \quad (20)$$

Then, we have

$$\begin{aligned} \int (y - f_{LS}(\mathbf{x}))^2 dp(\mathbf{x}, y) &= \int \int (y - f_{LS}(\mathbf{x}))^2 dp(y|\mathbf{x}) dp(\mathbf{x}) \\ &= \int \left[(1 - f_{LS}(\mathbf{x}))^2 p(1|\mathbf{x}) + (f_{LS}(\mathbf{x}) + 1)^2 p(-1|\mathbf{x}) \right] dp(\mathbf{x}), \end{aligned} \quad (21)$$

which implies that the minimizer of the equation (20) satisfies

$$f_{LS}^*(\mathbf{x}) = 2p(1|\mathbf{x}) - 1 = p(1|\mathbf{x}) - p(-1|\mathbf{x}). \quad (22)$$

The optimal Bayes classifier can be recovered by: $f_{Bayes}^*(\mathbf{x}) = \text{sign}(f_{LS}^*(\mathbf{x}))$. Indeed, $f_{LS}^* > 0$ if and only if $p(1|\mathbf{x}) > p(-1|\mathbf{x})$.

Similar to the equation (18), a weighted version of the optimal Bayes classifier for binary class rebalancing can be defined as:

$$f_{wBayes}^* = \arg \min_{f_{wBayes}: \mathcal{X} \rightarrow \{-1, 1\}} \int_{\mathcal{X} \times \{-1, 1\}} w(y) \mathbf{1}(f_{wBayes}(\mathbf{x}) - y) dp(\mathbf{x}, y), \quad (23)$$

where $w(y)$ indicates a weight. Similar to the equation (19), the solution is as follows:

$$f_{wBayes}^*(\mathbf{x}) = \begin{cases} 1 & \text{if } p(1|\mathbf{x}) w(1) > p(-1|\mathbf{x}) w(-1) \\ -1 & \text{otherwise} \end{cases}. \quad (24)$$

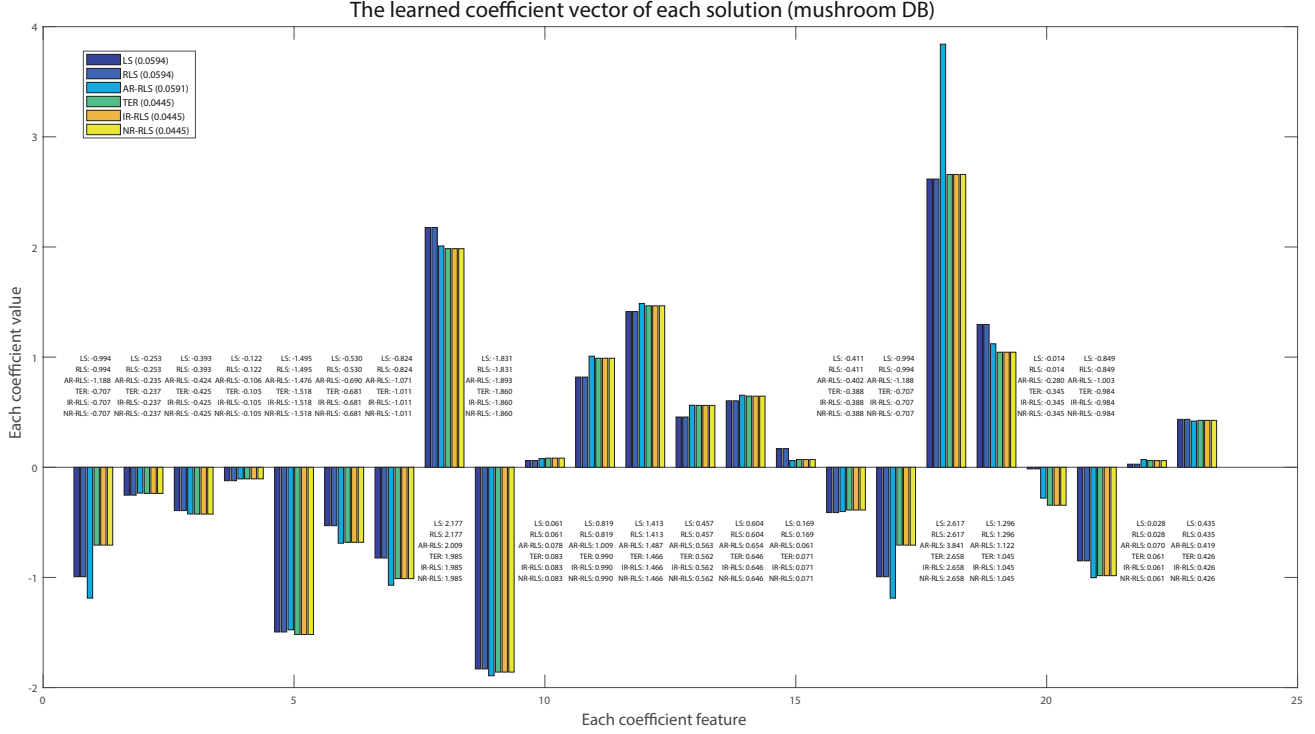


Figure 4. The learned coefficient vector of each algorithm in the ‘Mushroom’ data set.

By setting $w(1) = w(-1) = 0.5$, we can have the optimal Bayes classifier without the class rebalancing in the equation (19). Similar to the equation (20), the Weighted Least-Squares (WLS) minimization problem for the weighted optimal Bayes classifier is as follows:

$$f_{WLS}^* = \underset{f_{WLS}: \mathcal{X} \rightarrow \mathbb{R}}{\operatorname{argmin}} \int_{\mathcal{X} \times \{-1,1\}} w(y) (y - f_{WLS}(\mathbf{x}))^2 dp(\mathbf{x}, y). \quad (25)$$

Then, we have the minimizer of the equation (25) satisfies

$$f_{WLS}^*(\mathbf{x}) = \frac{p(1|\mathbf{x})w(1) - p(-1|\mathbf{x})w(-1)}{p(1|\mathbf{x})w(1) + p(-1|\mathbf{x})w(-1)}. \quad (26)$$

By assuming $w(1) > 0$ and $w(-1) > 0$, the weighted optimal Bayes classifier can be recovered by: $f_{wBayes}^*(\mathbf{x}) = \operatorname{sign}(f_{WLS}^*(\mathbf{x}))$. Therefore, $f_{WLS}^* > 0$ if and only if $p(1|\mathbf{x})w(1) > p(-1|\mathbf{x})w(-1)$.

Similar to the equation (25), the Total-Error-Rate (TER) minimization problem for the weighted optimal Bayes classifier is defined as:

$$f_{TER}^* = \underset{f_{TER}: \mathcal{X} \rightarrow \mathbb{R}}{\operatorname{argmin}} \int_{\mathcal{X} \times \{-1,1\}} w(-1) (y^- - f_{TER}(\mathbf{x}))^2 + w(1) (y^+ - f_{TER}(\mathbf{x}))^2 dp(\mathbf{x}, y), \quad (27)$$

where y^- and y^+ respectively are -1 and 1 for negative and positive classes. Similar to the equation (26), we have

$$f_{TER}^*(\mathbf{x}) = \frac{p(1|\mathbf{x})w(1) - p(-1|\mathbf{x})w(-1)}{p(1|\mathbf{x})w(1) + p(-1|\mathbf{x})w(-1)}. \quad (28)$$

Since $w(1) = \frac{1}{n^+} > 0$ and $w(-1) = \frac{1}{n^-} > 0$ in our work, the weighted optimal Bayes classifier can be recovered by: $f_{wBayes}^*(\mathbf{x}) = \operatorname{sign}(f_{TER}^*(\mathbf{x}))$. Therefore, $f_{TER}^* > 0$ if and only if $p(1|\mathbf{x})w(1) > p(-1|\mathbf{x})w(-1)$. Since the proposed NR-RLS classifier could exactly converge to the TER classifier, we conclude that the NR-RLS classifier can asymptotically recover the weighted optimal Bayes classifier.

Table 5. Highlighted summary of the 6 real-world data sets (e.g., the imbalance ratio < 0.5).

No.	DATA SETS	SIZE	DIMENSION	RATIO
4	WPBC	194	33	0.31
17	BLOOD-TRANSFUSION	748	4	0.31
22	OZONE-EIGHT	1,847	72	0.07
23	OZONE-ONE	1,848	72	0.03
30	IJCNN1	141,691	22	0.11
31	SKIN-NONSKIN	245,057	3	0.26

Table 6. Highlighted comparison of average G-means and (ranks).

No.	G-MEAN \pm STD (RANK)							
	THE FIRST-ORDER		THE SECOND-ORDER					
	PE	PA	CW	AROW	ACOG	RLS	AR-RLS	NR-RLS AND IR-RLS
4	0.440 \pm 0.093 (5)	0.440 \pm 0.075 (6)	0.522 \pm 0.087 (4)	0.285 \pm 0.230 (7)	0.114 \pm 0.176 (8)	0.639 \pm 0.081 (3)	0.687 \pm 0.058 (2)	0.688 \pm 0.047 (1)
17	0.485 \pm 0.046 (4)	0.456 \pm 0.040 (5)	0.526 \pm 0.057 (3)	0.237 \pm 0.100 (7)	0.103 \pm 0.139 (8)	0.286 \pm 0.043 (6)	0.682 \pm 0.023 (2)	0.685 \pm 0.022 (1)
22	0.364 \pm 0.066 (4)	0.296 \pm 0.061 (5)	0.571 \pm 0.045 (3)	0.072 \pm 0.106 (6)	0.000 \pm 0.000 (8)	0.007 \pm 0.029 (7)	0.807 \pm 0.033 (2)	0.820 \pm 0.018 (1)
23	0.240 \pm 0.104 (4)	0.161 \pm 0.101 (5)	0.423 \pm 0.100 (3)	0.009 \pm 0.041 (6.5)	0.009 \pm 0.041 (6.5)	0.000 \pm 0.000 (8)	0.788 \pm 0.036 (2)	0.819 \pm 0.035 (1)
30	0.631 \pm 0.004 (4)	0.627 \pm 0.005 (5)	0.692 \pm 0.004 (3)	0.508 \pm 0.009 (6)	0.173 \pm 0.085 (8)	0.301 \pm 0.007 (7)	0.858 \pm 0.004 (2)	0.859 \pm 0.004 (1)
31	0.768 \pm 0.002 (7)	0.783 \pm 0.002 (6)	0.454 \pm 0.015 (8)	0.899 \pm 0.001 (4)	0.784 \pm 0.342 (5)	0.904 \pm 0.001 (3)	0.957 \pm 0.000 (2)	0.958 \pm 0.000 (1)
AVG.	0.488 \pm 0.189 (4.66)	0.461 \pm 0.223 (5.33)	0.531 \pm 0.095 (4.00)	0.335 \pm 0.327 (6.08)	0.197 \pm 0.295 (7.25)	0.356 \pm 0.357 (5.66)	0.797 \pm 0.105 (2)	0.805 \pm 0.104 (1)

B. Extension to multiclass classification

The multiclass version of NR-RLS can be easily extended by the one-vs-all classification scheme as follows:

$$\Theta_t = [\mathbf{w}_t^1, \mathbf{w}_t^2, \dots, \mathbf{w}_t^c] \in \mathbb{R}^{d \times c}, \quad (29)$$

where c is the number of classes. Each solution, \mathbf{w}_t^j , is updated upon the arrival of the new training sample. The time complexity of the multiclass NR-RLS is $\mathcal{O}(2cd^2)$ which still has a constant time complexity since the number of classes will be fixed before training.

C. The learned coefficient vectors of each algorithm

In this appendix, we show the learned coefficient vectors after training all the input samples for the compared algorithms in Fig. 4. Each bracket in legends indicates the mean value of each coefficient vector. In this figure, the no weighting based group (e.g., LS and RLS) and the exact reweighting based group (e.g., TER, IR-RLS and NR-RLS) show equal coefficient values in each group whereas the approximate reweighting based AR-RLS show different coefficient values from the exact reweighting based group. This result further verifies the convergence of NR-RLS to its batch setting for TER minimization.

D. L_2 -norm, G -mean and CPU time values for each data set

In this appendix, we provide each plot of the L_2 -norm, the G -mean and the CPU time values for each data set which is not shown in the main paper. Due to the out-of-memory issue caused by the huge number of samples, the batch mode solutions (e.g., LS and TER) are omitted in the cod-rna, ijcn1 and skin-nonskin data sets. In all the figures, the same convergence results between LS and RLS are shown in the no weighting based group. Similarly, the same convergence results among TER, IR-RLS and NR-RLS are shown in the exact reweighting group whereas the convergence results of the approximate reweighting AR-RLS is different from the exact reweighting group.

E. Highlighted comparison on the highly imbalanced data sets

In Table 5 and 6, we selected the six data sets highly imbalanced (e.g., the imbalance ratio < 0.5) to feel the impact of the reweighting based online classifiers. We can see that the exactly reweighted NR-RLS and IR-RLS are seen to be the best performer, while the approximately reweighted AR-RLS is the second best performer. Many of the other algorithms that have no reweighting scheme, suffer from the highly imbalanced data sets (e.g., specially the data set no. 17, 22, 23 and 30).

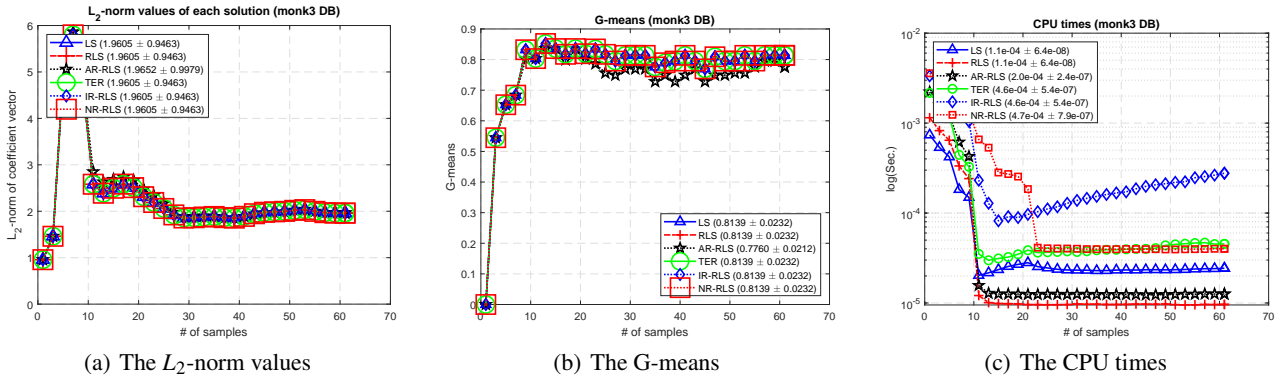


Figure 5. Monk-3 DB

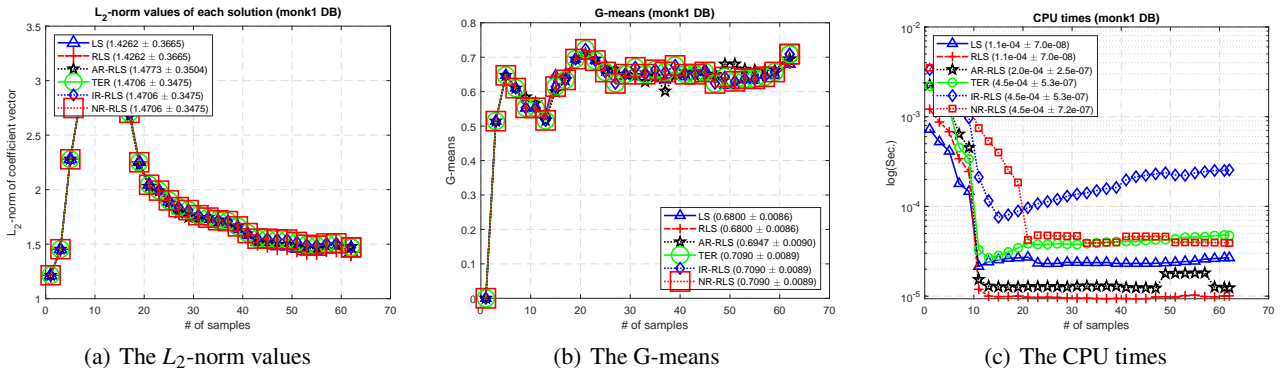


Figure 6. Monk-1 DB

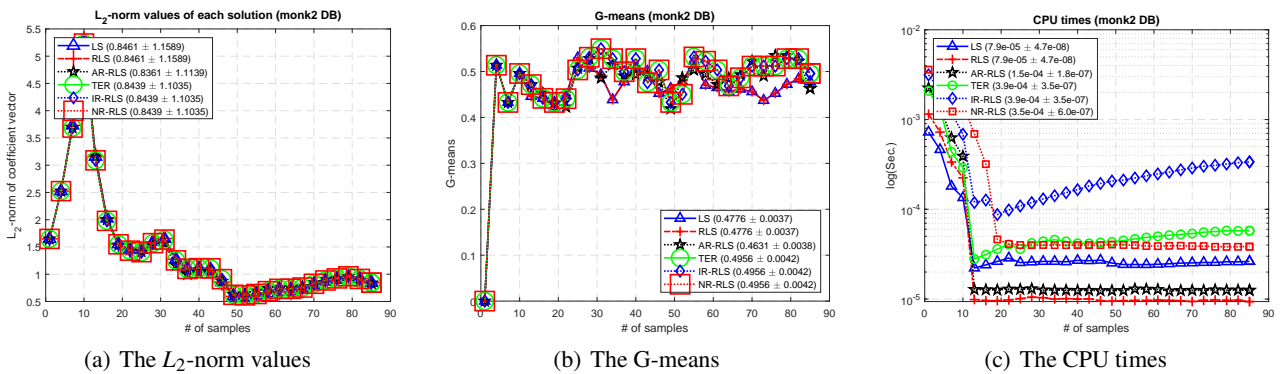


Figure 7. Monk-2 DB

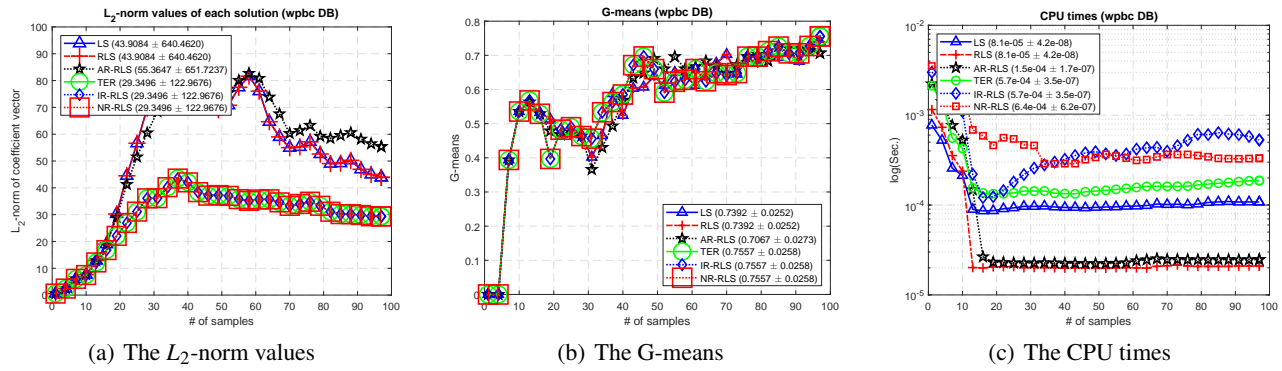


Figure 8. Wpbc

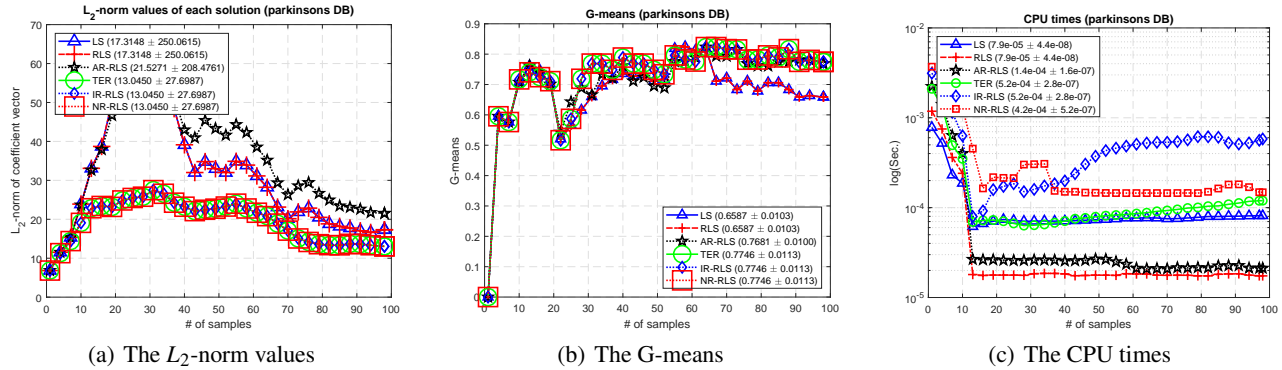


Figure 9. Parkinsons

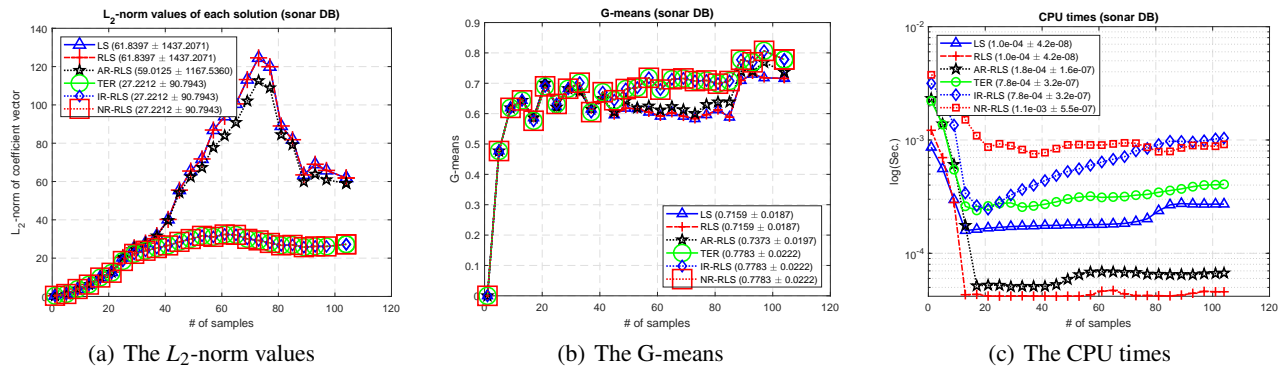


Figure 10. Sonar

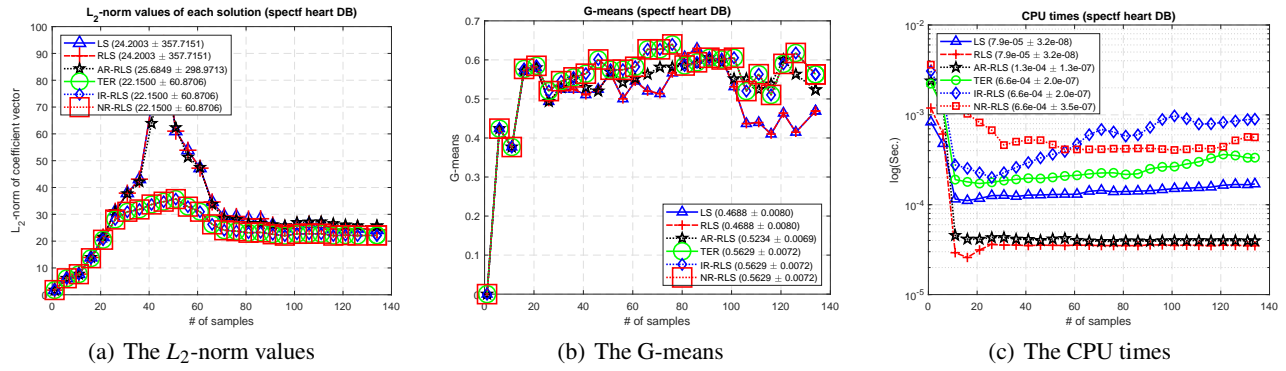


Figure 11. SPECTF-heart

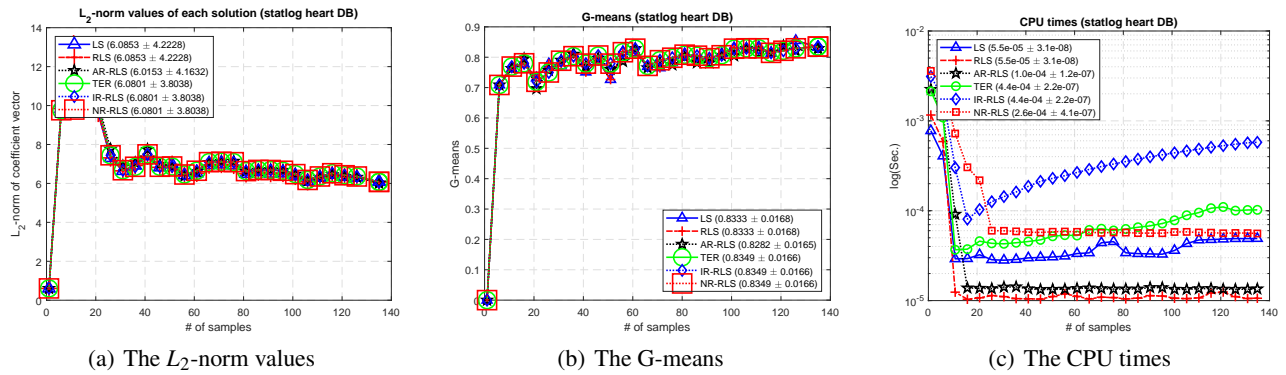


Figure 12. StatLog-heart

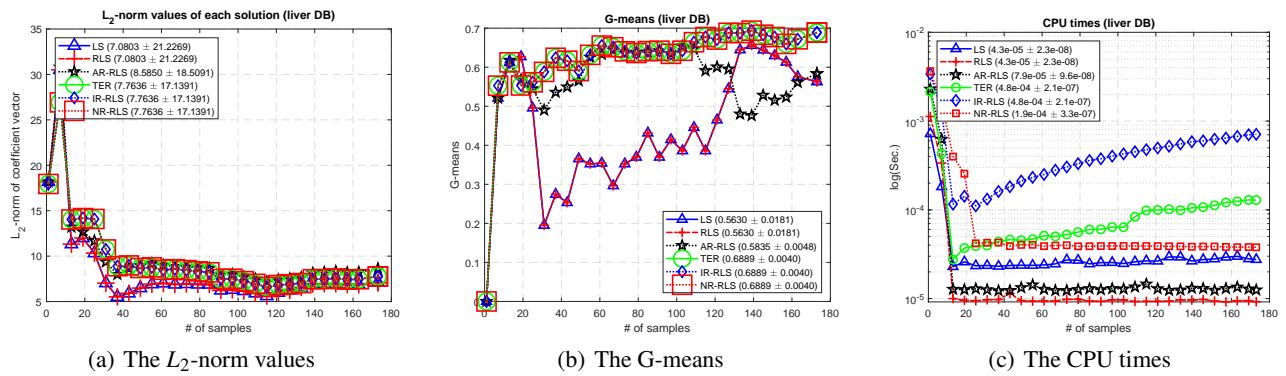


Figure 13. BUPA-liver

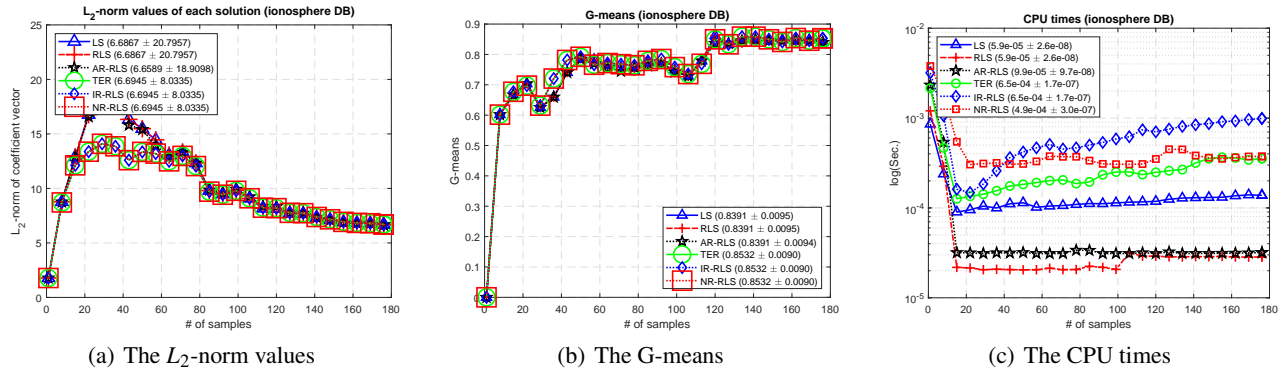


Figure 14. Ionosphere

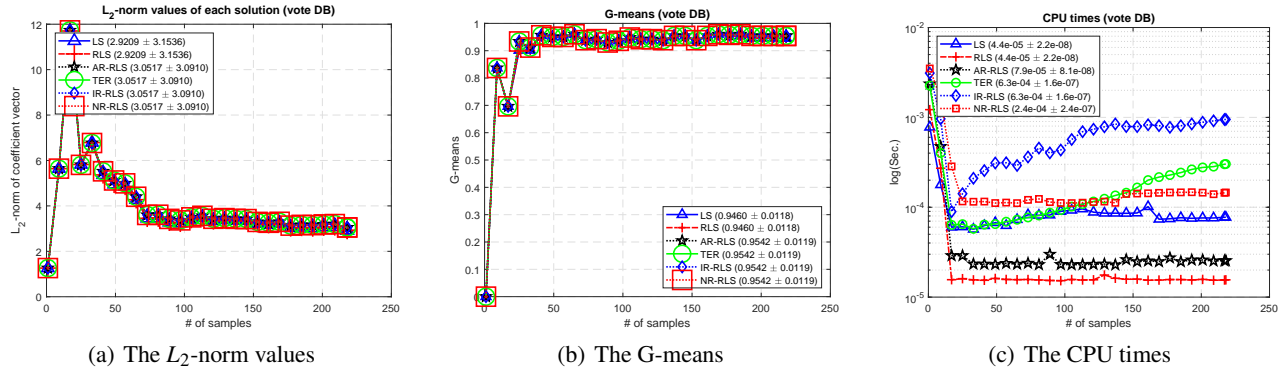


Figure 15. Votes

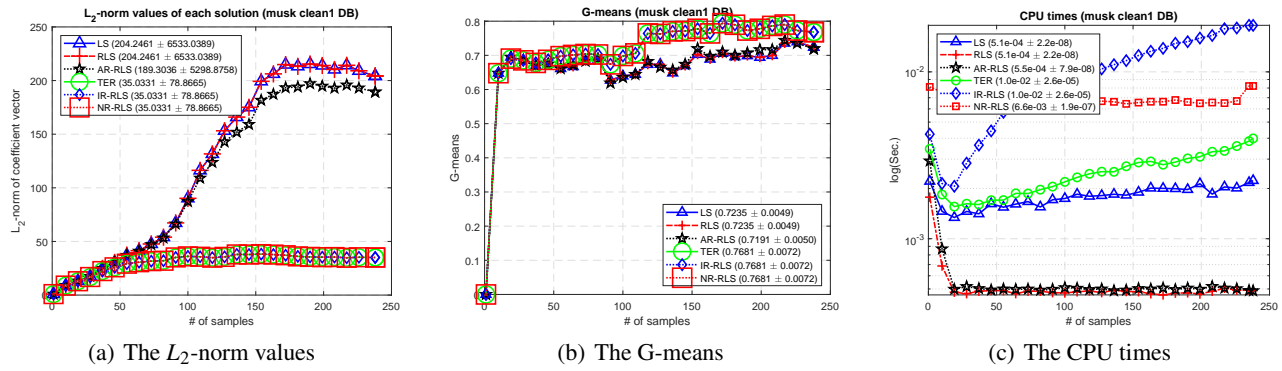


Figure 16. Musk-clean-1

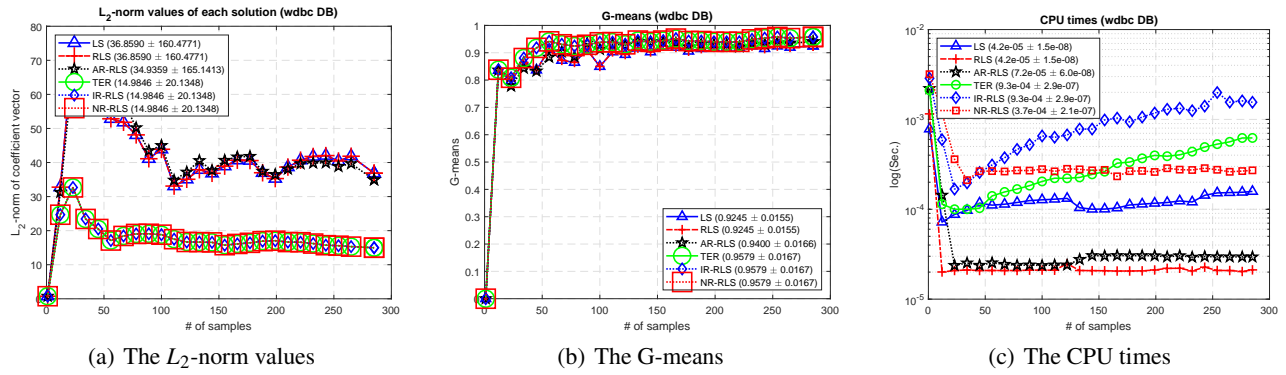


Figure 17. Wdbc

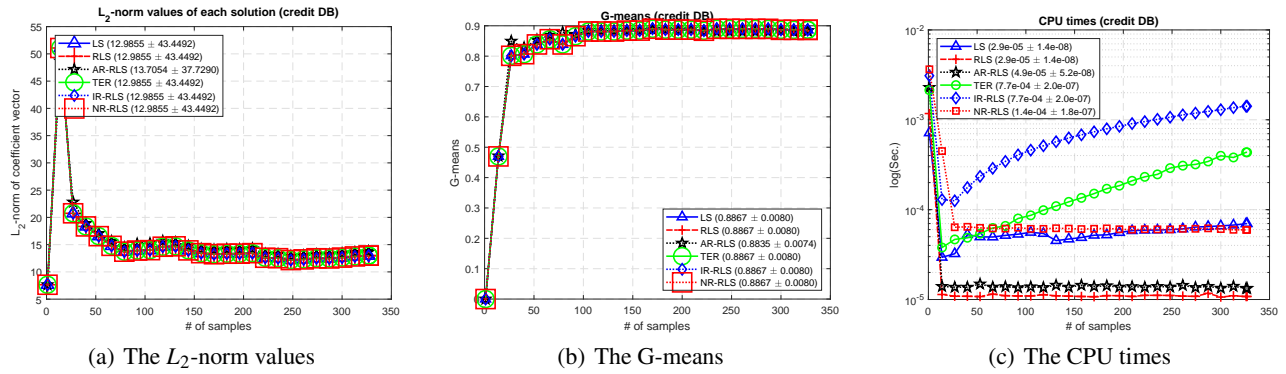


Figure 18. Credit-app

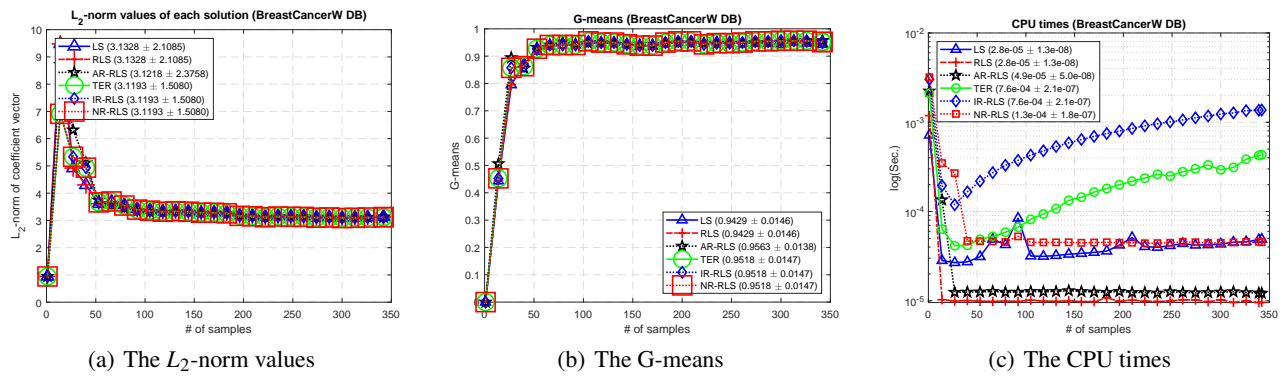


Figure 19. Breast-cancer-W

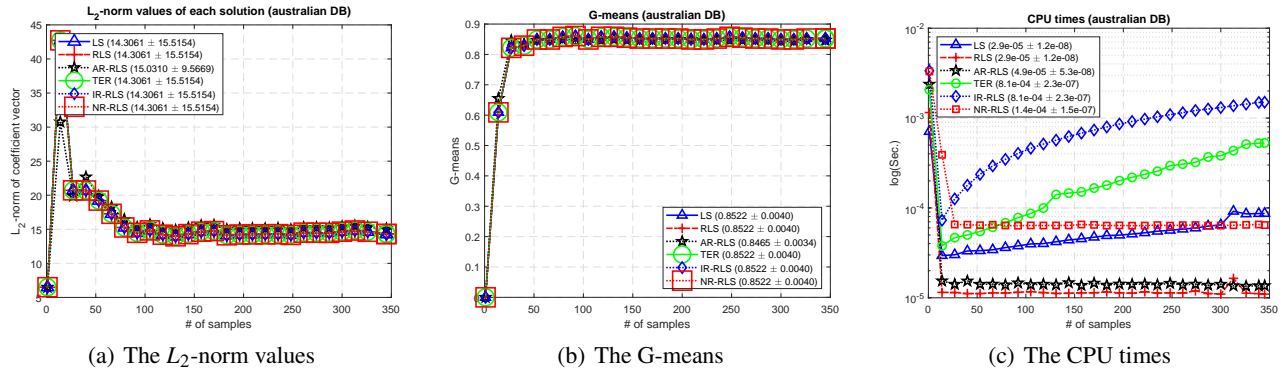


Figure 20. Statlog-australian

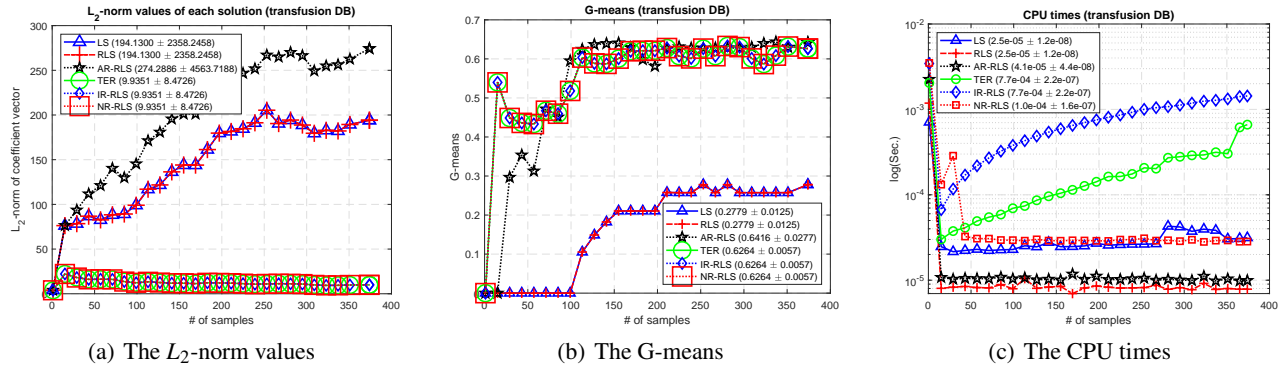


Figure 21. Blood-transfusion

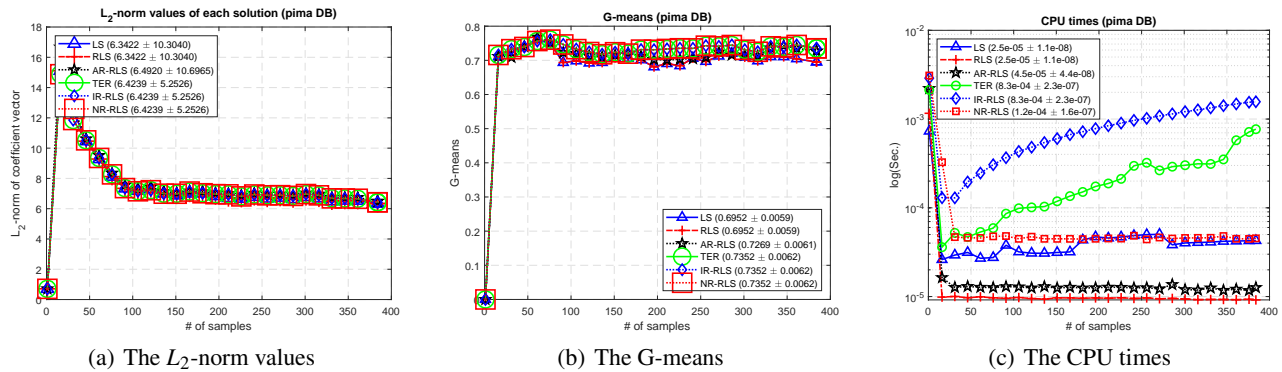


Figure 22. Pima-diabetes

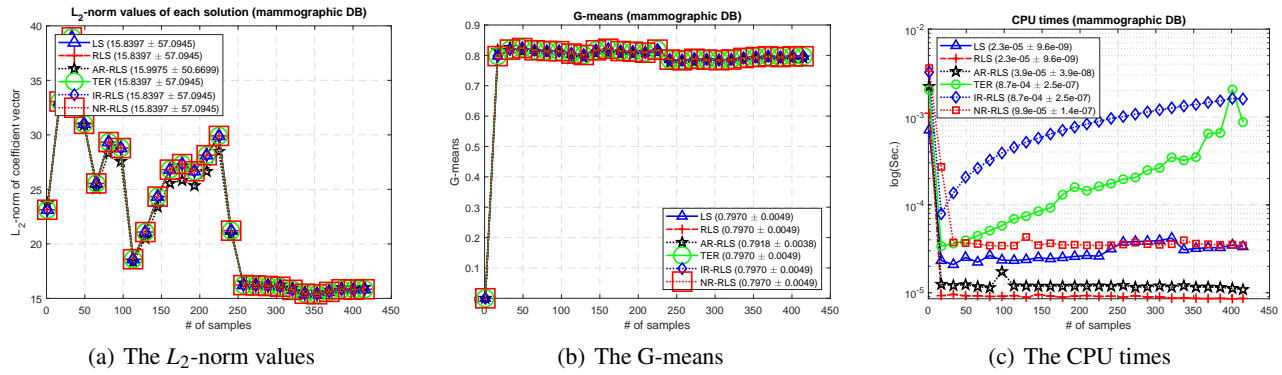


Figure 23. Mammographic

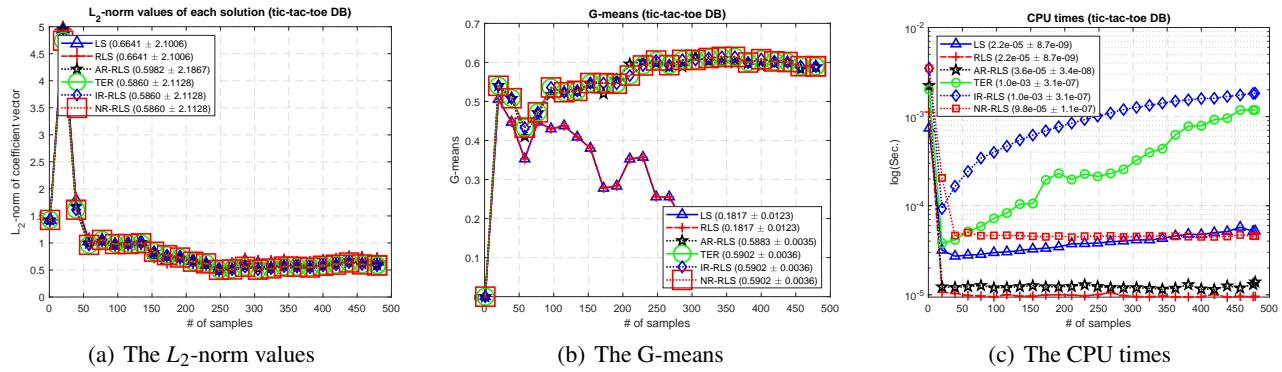


Figure 24. Tic-tac-toe

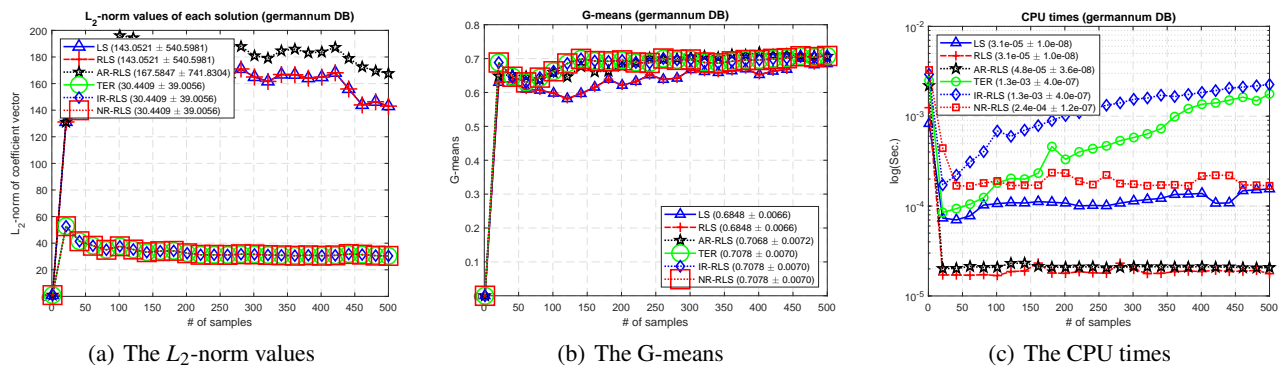


Figure 25. Statlg-german

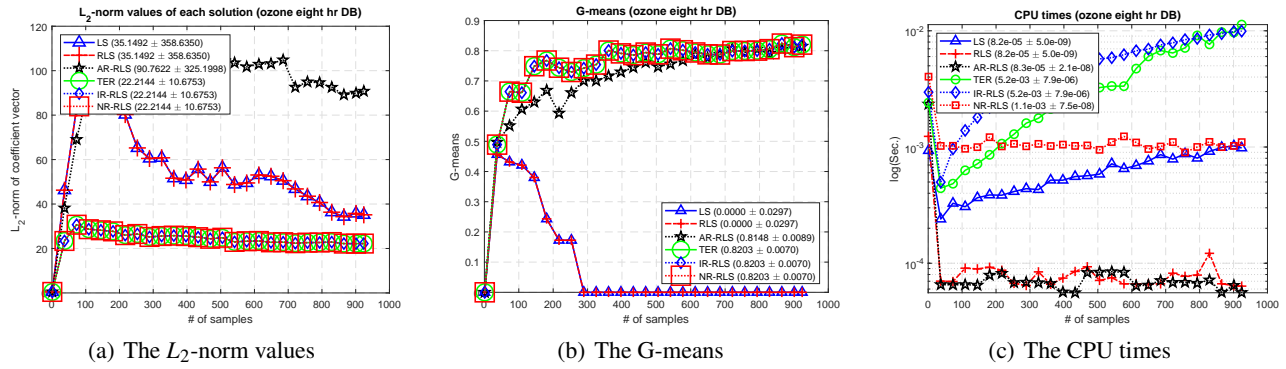


Figure 26. Ozone-eight

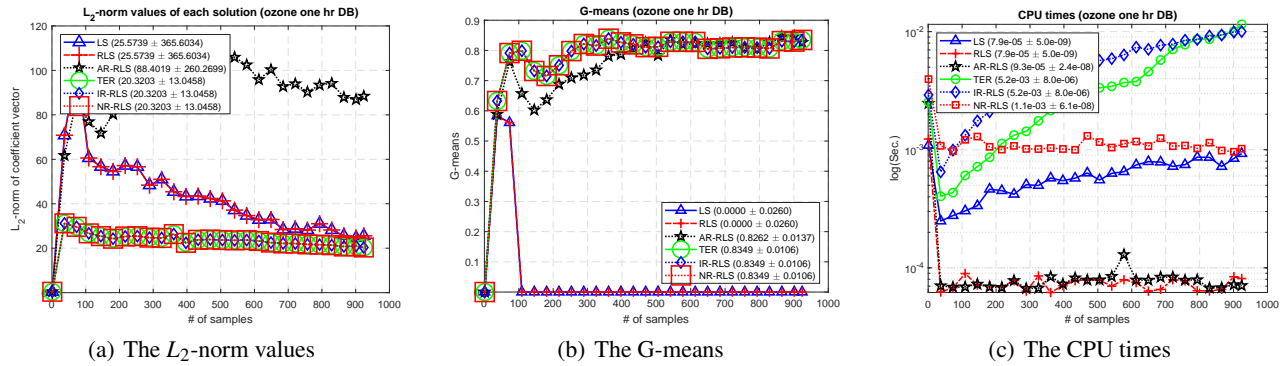


Figure 27. Ozone-one

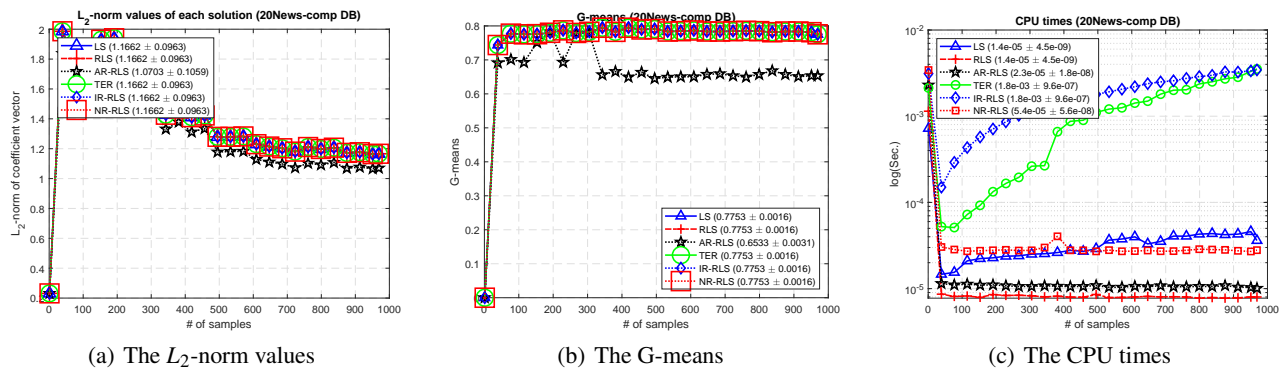


Figure 28. 20News-comp

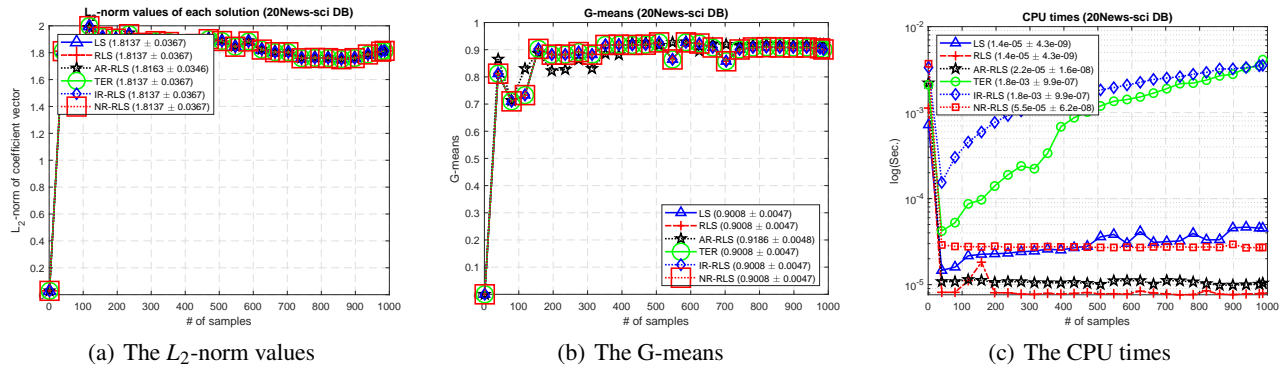


Figure 29. 20News-sci

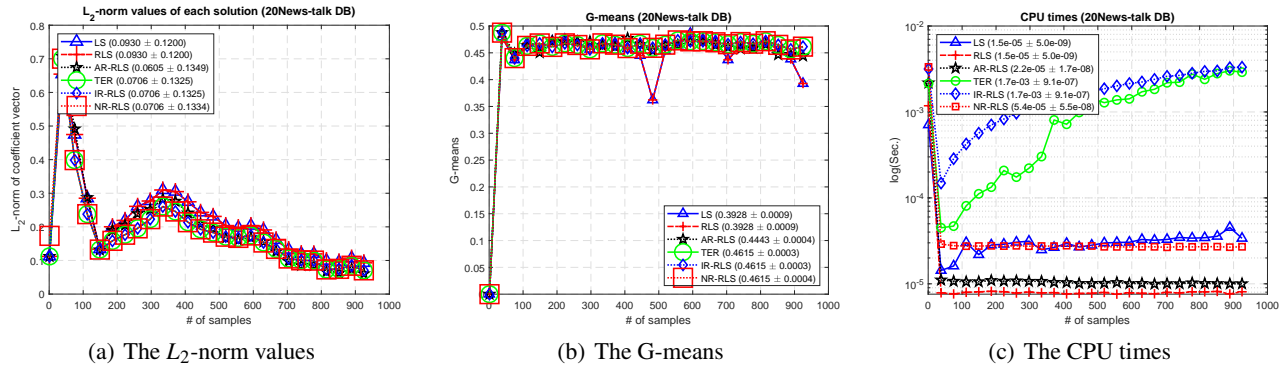


Figure 30. 20News-talk

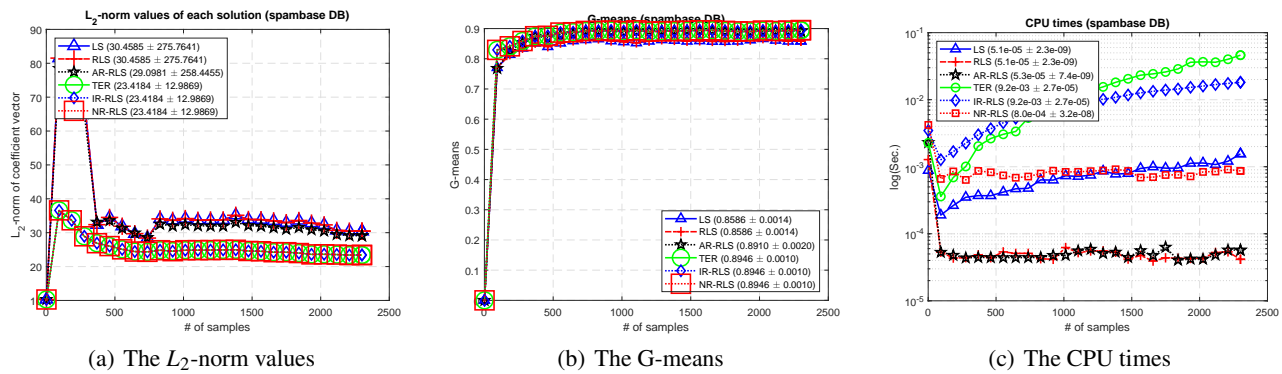
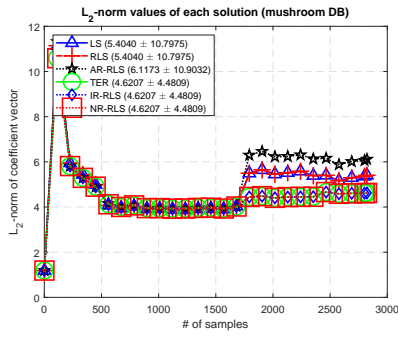
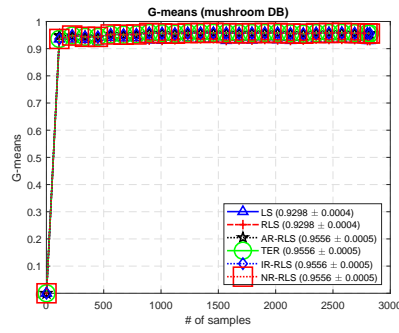


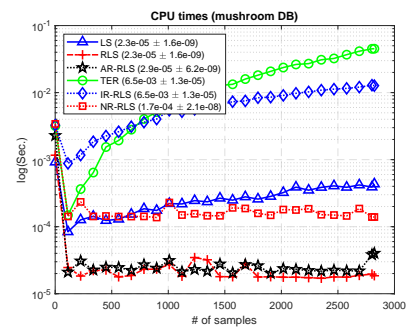
Figure 31. Spambase



(a) The L_2 -norm values

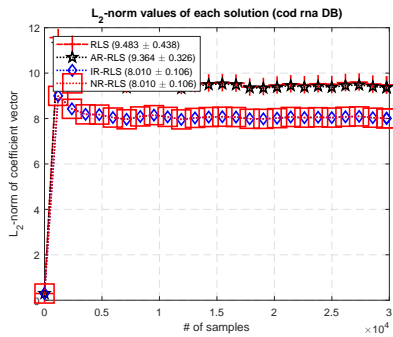


(b) The G-means

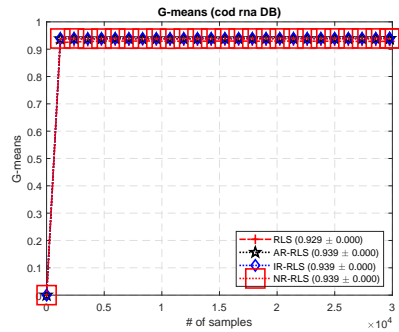


(c) The CPU times

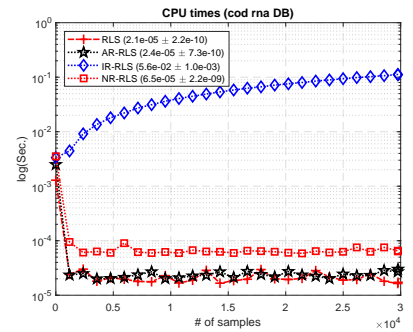
Figure 32. Mushroom



(a) The L_2 -norm values

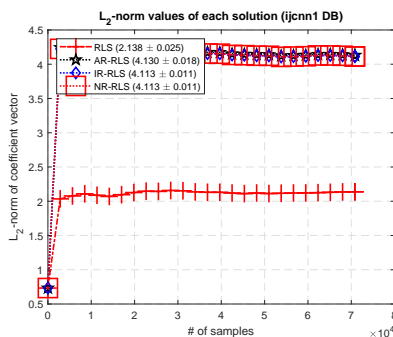


(b) The G-means

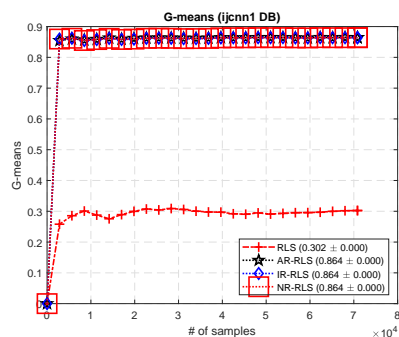


(c) The CPU times

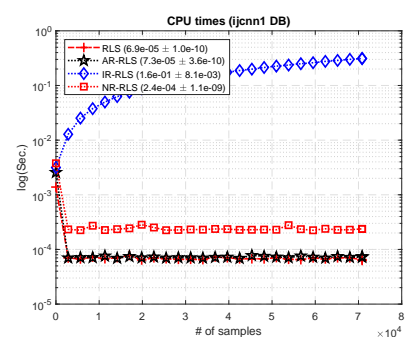
Figure 33. Cod-rna



(a) The L_2 -norm values



(b) The G-means



(c) The CPU times

Figure 34. Ijcnn1

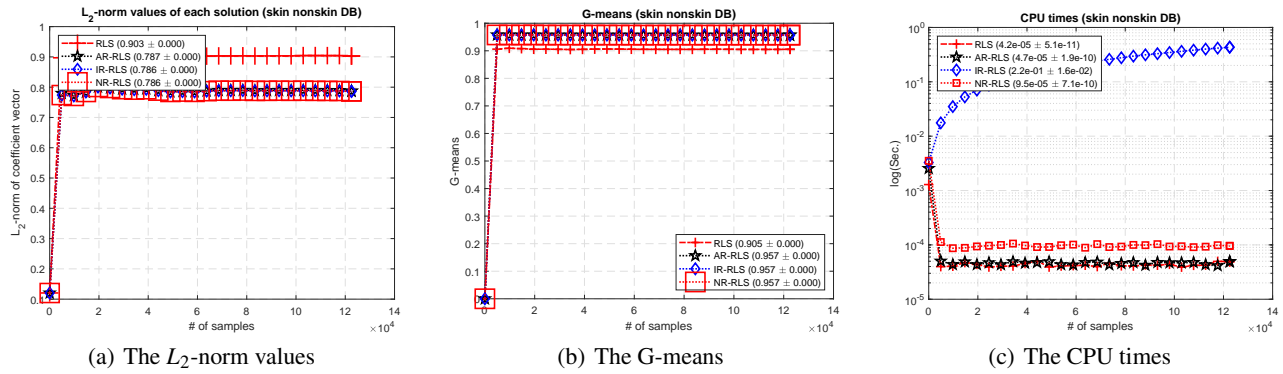


Figure 35. Skin-nonskin